

SOLAR SHADOW MAPS

by

Christopher Duffield

---

A Thesis Submitted to the Faculty of the

DEPARTMENT OF GEOSCIENCES

In Partial Fulfillment of the Requirements  
For the Degree of

MASTER OF SCIENCE

In the Graduate College

THE UNIVERSITY OF ARIZONA

1 9 7 5

STATEMENT BY AUTHOR

This thesis has been submitted in partial fulfillment of requirements for an advanced degree at The University of Arizona and is deposited in the University Library to be made available to borrowers under rules of the Library.

Brief quotations from this thesis are allowable without special permission, provided that accurate acknowledgment of source is made. Requests for permission for extended quotation from or reproduction of this manuscript in whole or in part may be granted by the head of the major department or the Dean of the Graduate College when in his judgment the proposed use of the material is in the interests of scholarship. In all other instances, however, permission must be obtained from the author.

SIGNED: Christopher Duffield

APPROVAL BY THESIS DIRECTOR

This thesis has been approved on the date shown below:

William B. Bull

W. B. BULL

Professor of Geosciences

December 1, 1975  
Date

## ACKNOWLEDGMENTS

The following people and departments at The University of Arizona deserve credit and special thanks for their assistance in various phases of this research:

Thesis advisor William B. Bull and thesis committee Laurence M. Gould, Dietmar Schumacher, and Terah L. Smiley for encouragement, thoughtful criticism, and careful reading of this manuscript.

Department of Geosciences for generous support and use of facilities.

Dr. William D. Sellers for help and access to solar radiation records of the Institute of Atmospheric Physics.

James M. Palmer, Optical Sciences graduate student, for designing and helping construct a radiometer used for this and other studies.

Dean Robert E. McConnell, College of Architecture, for access to a Heliolux sun machine.

The Library Map Collection staff for lending plastic raised-relief maps.

And the Office of Arid Lands Studies for computer outputs (used for literature survey) from two information systems, the Arid Lands Information System (ALIS) and Oak Ridge National Laboratory's RECON system.

## TABLE OF CONTENTS

	Page
LIST OF ILLUSTRATIONS . . . . .	vi
LIST OF TABLES . . . . .	viii
ABSTRACT . . . . .	ix
1. INTRODUCTION . . . . .	1
Overview . . . . .	1
Geometric Assumptions . . . . .	2
Geometric Definitions . . . . .	3
2. PREVIOUS SHADOW ANALYSIS TECHNIQUES . . . . .	6
Insolation on a Horizontal Surface . . . . .	6
Slope Shade . . . . .	7
Projected Shade and Slope Shade for a Point . . . . .	7
Projected Shade and Slope Shade for an Area . . . . .	8
Geometric Projection . . . . .	8
Topographic Profiling . . . . .	9
Computer Techniques . . . . .	9
Architectural Model Illumination:	
Sun Machines . . . . .	10
Architectural Model Illumination:	
Sundials . . . . .	11
Miscellaneous Shadow Techniques . . . . .	12
Direct Observation . . . . .	12
SLAR and Pseudo-SLAR . . . . .	12
Sundials . . . . .	13
3. NEW SHADOW MAPPING TECHNIQUE . . . . .	14
General Description . . . . .	14
Apparatus . . . . .	15
Shadow Dial Geometry . . . . .	17
Procedure . . . . .	19
Discussion . . . . .	20
Alternative Uses . . . . .	21

TABLE OF CONTENTS--Continued

	Page
4. MOHAWK MOUNTAINS STUDY . . . . .	23
Introduction . . . . .	23
Shadow Calibration Units . . . . .	25
Accuracy and Error . . . . .	27
Sample Shadow Maps . . . . .	29
Shadow Implications . . . . .	39
5. APPLICATIONS . . . . .	41
Preview . . . . .	41
Microclimatic Systems . . . . .	42
Hydrologic Systems . . . . .	43
Geological Systems . . . . .	44
Biological Systems . . . . .	46
Plant Physiology . . . . .	46
Plant Geography and Ecology . . . . .	47
Cultivated Plants . . . . .	47
Animals . . . . .	48
Human and Industrial Systems . . . . .	48
Aesthetics and Ritual . . . . .	48
Archaeology, Architecture, and Urban Planning . . . . .	49
Recreation . . . . .	50
Solar Technology . . . . .	51
Legal Aspects . . . . .	51
Industrial Ecology . . . . .	52
APPENDIX A: SOLAR RADIATION MODEL FOR SOUTHERN ARIZONA ATMOSPHERE . . . . .	54
APPENDIX B: SOLAR RADIATION MODEL FOR MOHAWK MOUNTAINS . . . . .	63
APPENDIX C: TOTAL ENERGY BLOCKED BY SHADOWS . . . . .	69
REFERENCES . . . . .	71

## LIST OF ILLUSTRATIONS

Figure	Page
1. Topographic Shade = Slope Shade + Projected Shade . . . . .	4
2. Solar shadow mapping apparatus . . . . .	16
3. Shadow dial, perspective view . . . . .	18
4. Shadow dial pattern for Mohawk Mountains study . . . . .	18
5. Mohawk Mountains topographic map . . . . .	24
6. Mohawk Mountains shadow map accuracy check . . . . .	28
7. Mohawk Mountains shadow map: June 21 (summer solstice) . . . . .	30
8. Mohawk Mountains shadow map: May 21, July 21 . . . . .	31
9. Mohawk Mountains shadow map: April 21, August 21 . . . . .	32
10. Mohawk Mountains shadow map: March 21, September 21 (equinoxes) . . . . .	33
11. Mohawk Mountains shadow map: February 21, October 21 . . . . .	34
12. Mohawk Mountains shadow map: January 21, November 21 . . . . .	35
13. Mohawk Mountains shadow map: December 21 (winter solstice) . . . . .	36
14. Mohawk Mountains shadow map: annual envelopes . . . . .	38
15. Solar elevation angle vs. time: Tucson, July 10 . . . . .	57
16. Solar radiation parameters vs. time: Tucson, Ariz., July 10, 1974 . . . . .	60

LIST OF ILLUSTRATIONS--Continued

Figure		Page
17.	Solar radiation parameters vs. solar elevation angle: general model . . . . .	61
18.	Solar elevation angle vs. time: monthly curves, 32° north . . . . .	65
19.	Direct solar radiation (Q) vs. time: monthly curves, 32° north . . . . .	66
20.	Cumulative direct solar radiation vs. time: monthly curves, 32° north . . . . .	67
21.	Area shaded vs. cumulative direct solar radiation blocked: June 21 . . . . .	70

LIST OF TABLES

Table	Page
1. Solar radiation data: Tucson, Ariz., July 10, 1974 . . . . .	58
2. Solar radiation parameter values for selected solar elevation angles . . . . .	62
3. Elevation angles and times for selected Qt values . . . . .	68

## ABSTRACT

A simple, rapid, and inexpensive new analog technique has been developed for mapping outlines of shadows cast by topographic features under direct sunlight. A small raised-relief model is illuminated from simulated sun angles for specific dates and times. Illumination angle is adjusted for vertical exaggeration of the model. Shadows are photographed and their outlines are transferred to a base map. Shadow boundaries can be determined graphically (tedious), or by digital computer. But this new analog method can effortlessly and instantaneously process the vast amounts of topographic data already stored in raised-relief format, and offers an option where computers are unavailable or too costly. Monthly maps of shadows for various times of the day were prepared by this method for part of the Mohawk Mountains, Yuma County, Arizona. If a denudation rate of 5 centimeters per thousand years is assumed then these shadow patterns have not changed significantly in 500,000 years. Shadow maps can help in evaluating time and space variations of direct solar radiation, which can strongly influence a wide variety of microclimatic, hydrologic, geological, biological, and industrial systems.

## CHAPTER 1

### INTRODUCTION

#### Overview

On the macro-scale, our planet's solar shadow pattern is quite simple. Half the spheroid is illuminated by the sun, half is in shade. And the indistinct terminator separating the halves sweeps the surface in regular daily and seasonal cycles. On the micro-scale, however, interplay between direct sunlight and the diverse and ever-changing atmospheric and surface forms produces shadow patterns which are infinitely more complex and range in size from kilometers to microns.

Fleeting topographic shadows (solar shadows cast by topographic forms), never still, are among the most intricate, dynamic, and fascinating features of any landscape. Yet, despite apparent complexity, their motions reflect with precision and in miniature the simple diurnal and annual celestial clockwork cycles of the earth-sun orbital system.

At any instant the boundaries of these shadows partition sharply contrasting visual fields. But, more important, they also define distinctly different energy

domains, with profound influence on numerous radiant energy-dependent phenomena.

"NEQUE LUX SINE UMBRA" (Light cannot be without shade), advises an old sundial motto (Hogg 1917). It is clear that solar shadows (the absence of direct sunlight) must affect the very same set of phenomena which direct sunlight affects, although inversely. And such phenomena range widely, from photosynthesis to air temperature, from sunbathing on a Puerto Rican beach to snowmelt and permafrost depth in Alaska.

Knowledge of topographic shadows is thus quite relevant to the work of many professionals in numerous fields. I hope this report will benefit these people by bringing new light to the ancient subject of solar shadow studies.

After reviewing previous shadow mapping techniques, this paper presents a new method and applies it to a desert mountain range in southwestern Arizona. The final section surveys some possible fields for practical application of solar shadow mapping.

#### Geometric Assumptions

As do most studies of solar radiation effects at the earth's surface, this report neglects minor long-term perturbations in the earth-sun planetary system (obliquity of ecliptic, orbital eccentricity, and precession of

equinoxes). Direct sunlight is assumed to travel in parallel rays, since apparent solar angular diameter is small. Atmospheric refraction is ignored as insignificant, and diffuse (sky) radiation is not considered.

### Geometric Definitions

Shadow projection (sciagraphy) by parallel rays is known geometrically as affine transformation, and such projection onto a curved, irregular surface is called topological transformation (March and Steadman 1971). Topographic shadows, then, are affine topological transformations of topographic forms.

"Umbra" is used as Randall (1902) defined it: "that portion of space excluded from the light by an opaque body." I use "shadow" to mean the specific, concrete intersection of an umbra with a surface. "Shading" is the process of shadow projection, and "shade" is the abstract existence of shadow(s).

The use by various authors of two levels of shadow mapping completeness (discussed in next section) points out the need to distinguish between two types or components of topographic shade. I suggest that these types be called "slope shade" and "projected shade". They are illustrated in Figure 1.

Slope shade occurs when a surface element would in isolation shade itself (would be in its own umbra).

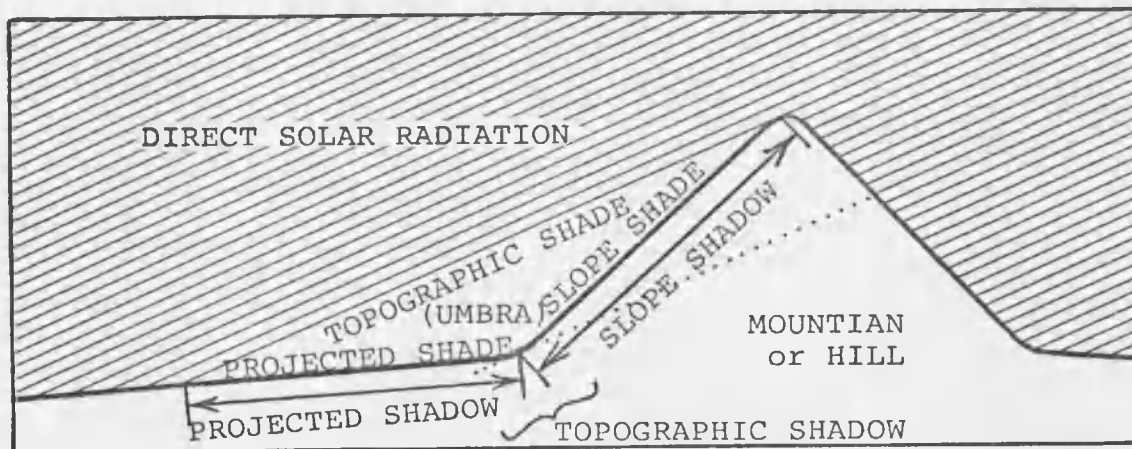


Figure 1. Topographic Shade = Slope Shade + Projected Shade

The normal to such an element is more than 90 degrees from solar illumination direction. Another way to express this relationship is:

$$\tan E < \sin A \cdot \tan S$$

(derived from Wise 1969a), where E is solar elevation angle, A is angle between slope strike and solar azimuth, and S is slope dip. A "slope shadow" consists of one or more contiguous elements in slope shade.

Projected shade occurs when a surface element, which in isolation would be illuminated, is shaded by (is in the umbra of) another slope element. In this case the surface normal is less than 90 degrees from sunlight direction ( $\tan E > \sin A \cdot \tan S$ ). One or more contiguous elements in projected shade constitute a "projected shadow".

Topologically, for a single continuous surface, slope shadows and projected shadows must always coexist and border each other (except when a slope is entirely parallel to solar rays). Either can surround the other, but the outer boundary of a shaded area must touch both types of shadow. Slope shadow is completely bounded by points where solar illumination direction is tangent to the surface ( $\tan E = \sin A \cdot \tan S$ ).

## CHAPTER 2

### PREVIOUS SHADOW ANALYSIS TECHNIQUES

#### Insolation on a Horizontal Surface

Topographic shade is usually studied in terms of the direct solar radiation that is blocked either instantaneously or cumulatively. Topographic shade investigations are thus generally based on simple mathematical solar radiation models which ignore topography. In these basic models, direct solar radiation on a unit horizontal surface is usually a simple function of apparent sun position (illumination direction), which is a function of geographic coordinates, seasonal declination, and hour angle.

Some such models ignore atmospheric effects (e.g., Sellers 1965), and yield values of "potential" or "extraterrestrial" insolation. Others (e.g., Robinson 1966) take atmospheric absorption and scattering of light into account. All these models automatically allow for what might be called "global shade", the shade of the night hemisphere.

When topographic shadow effects are superimposed on these models, two levels of mapping completeness (mentioned earlier) are possible. Some studies map only slope shade; others map both slope shade and projected shade.

### Slope Shade

Slope insolation models yield values of direct solar radiation on unit slopes and automatically allow for slope shade. Slope strike and dip (or aspect and slope) are the input variables added to horizontal-surface insolation models. Slope model techniques can produce regional slope insolation or slope shade maps by analyzing each slope element separately. Projected shade (more difficult to determine because elevations of the numerous slope elements must be compared) is often neglected as smaller in magnitude and not worth the extra effort to map.

Slope insolation studies which ignore atmospheric effects include those by Fons, Bruce, and McMasters (1960), Lee (1963, 1964), and Sellers (1965). Investigations which assume specific atmospheric properties have been made by Nash (1963), Robinson (1966), Ohmura (1968), Fuggle (1970), and Buffo, Fritschen, and Murphy (1972). In contrast to static atmospheric assumptions in these studies, Garnier and Ohmura (1969) and Wilson (1970) used dynamic input of actual horizontal-surface insolation data from a field instrument.

### Projected Shade and Slope Shade for a Point

Topographic shade (combination of projected shade and slope shade) is easily evaluated for a single location by comparing skyline obstructions (above horizon) with

apparent sun position. This is done graphically by plotting both skyline and apparent sun paths on a single stereographic projection of the sky vault hemisphere. Duration of shade is determined from the resulting diagram, and can be input for either slope or horizontal-surface insolation models.

Skyline configuration can be determined by several methods. Geiger (1965) suggested the use of a theodolite at the site. Pleijel (1954, 1963) and Olgyay and Olgyay (1957) illustrated the use of whole-sky photographs made by convex mirror or fish-eye lens. And Ohmura (1970) outlined a technique for graphical reconstruction of skyline shape from a topographic map.

### Projected Shade and Slope Shade for an Area

#### Geometric Projection

Shadow projections of very simple geometric forms may be useful where topography approaches such simplicity, and may help comprehension of actual shadows where topography is more complex. The Puerto Rico Planning Board (1969) published diagrams of shadows cast by an idealized square tower and by a vertical pole onto a horizontal surface. And Knowles (1974) presented drawings of zones of influence of shadows cast by a vertical pole onto slopes of various orientations.

### Topographic Profiling

Garnett (1935) presented and applied a graphical technique for shadow map construction using topographic maps, and Lee (1963, 1964) also applied it. Topographic profiles are constructed for regularly-spaced lines parallel to solar azimuth, and shaded segments are defined on these profiles by projection lines parallel to solar elevation angle (as in Figure 1). Shadow areas are then mapped by connecting shaded segments on adjacent profiles. Although simple, this method is tedious and time-consuming.

### Computer Techniques

Various computer programs have been devised to automate and speed determination of topographic shade (especially with its more complex projected shade component). Ohmura (1970) described the computer storage of skyline obstruction data determined graphically by hand for each point of a map grid. The skyline data is automatically compared with apparent sun position during machine calculation of slope insolation. Garnier and Ohmura (1968, 1970) applied this method. Another computer program, designed for architects by Hosni (1971), makes geometric shadow projections of simple building forms, but is probably not well-suited to studies of complex natural topography.

More sophisticated techniques have been developed since 1970 for shadow projection by automatic topographic

profiling (removing the tedium from Garnett's (1935) method. Andrews (1971) and Williams, Barry, and Andrews (1972) applied such a technique using a square grid of map points. A similar method, but using triangular slope facets, was presented by Lecarpentier (1974). Computer techniques are convenient if computer time is available, but they require time-consuming (and somewhat tedious) digitization of topographic data.

#### Architectural Model Illumination: Sun Machines

Architects frequently build small-scale three-dimensional study models of proposed structures. It is not surprising that they have developed accurate techniques for studying and photographing sunlight and shade patterns and effects on these models. Numerous devices ("sun machines") have been designed to illuminate architectural models from simulated sun angles, automatically adjusting for any latitude, declination, and hour angle.

Olgay and Olgay (1957) described 30 types of sun machines in existence that year. Aronin (1953) and Taylor (1971) also discussed these devices. Sun machines can be divided into three categories: 1) those in which the model is fixed and the light moves (e.g., "Solarscope"), 2) those in which the model moves and the light is fixed (e.g., "Heliolux"), and 3) those in which both model and light move (e.g., "Heliodon"). Knowles (1974), taking a slightly

different approach, put a camera in place of the lamp on a Heliodon in order to determine which parts of a structure are illuminated and the magnitude of insolation on them (proportional to area on photograph). Sun machines are easy to use, but are unwieldy and expensive. Furthermore, most of them produce divergent light rays, resulting in reduced shadow projection accuracy.

#### Architectural Model Illumination: Sundials

Another, simpler technique has been developed by architects for model illumination. The model and a sundial are mounted on a platform, which represents a horizontal surface. The platform is tilted and turned until the sundial shadow is in the desired position and the model illumination direction corresponds to that for a specific latitude, date, and hour. An advantage of this method is that direct sunlight (with nearly parallel rays) can be used for illumination.

Possible sundial configurations are infinite (Rohr 1965). Pleijel developed a convenient "Little Sundial" in the form of a concave square box with sloping sides and a straight pin gnomon, or pointer (Aronin 1953, Olgyay and Olgyay 1957, Pleijel 1963). Separate dials were constructed for every two degrees latitude. Olgyay and Olgyay (1957) designed a more versatile "Shade Dial" which is readily adjusted for any latitude.

Publications which display topographic shadow maps, but which do not give details about techniques used, include those by Lee and Baumgartner (1966) and Knowles (1969).

### Miscellaneous Shadow Techniques

#### Direct Observation

The most straightforward method of studying topographic shadows is to observe them directly as they occur in nature. This can be done from the surface or from an aircraft or satellite. Although numerous photographs have shown topographic shadows, no systematic shadow studies have been done photographically (to my knowledge). It would clearly be expensive and take a long time to obtain comprehensive hourly, daily, and seasonal photo coverage.

Under the category of direct observation we might include the hourly and seasonal solar shadow sequence paintings by French impressionist Claude Monet in his "Haystack" and "Rouen Cathedral" series (Seitz 1960).

Perhaps also relevant here, at least one photogrammetric technique has been developed (Love 1966) to deduce topography from the shadows it casts--shadow mapping in reverse.

#### SLAR and Pseudo-SLAR

Another technique for producing and recording topographic shadows is side-looking airborne radar (SLAR).

With SLAR the landscape is illuminated from any desired angle by diverging microwaves from an artificial airborne source. A much simpler, faster, less expensive way to achieve remarkably similar results was developed and applied by D. U. Wise (1969a, 1969b), who produced numerous "pseudo-SLAR" images by illuminating detailed plastic relief maps from appropriate angles and photographing them from above.

### Sundials

Probably the most ancient field of systematic shadow study and application is the design and calibration of sundials. Earliest recorded sundials were made in Egypt around 1450 B.C. (Rohr 1965). Sundial geometries are diverse, but are generally simple (never approaching landscape complexity) for practical ease of calibration and observation.

## CHAPTER 3

### NEW SHADOW MAPPING TECHNIQUE

#### General Description

Juxtapose two of the shadow analysis techniques just discussed: simulating sunlight on architectural scale models, and making pseudo-SLAR images from illuminated plastic raised-relief maps. The possibility of a new technique, combining aspects of both, becomes immediately obvious. Why not model topographic shade by illuminating raised-relief maps from simulated sun angles?

The method as I have developed it is a simple, rapid procedure using an uncomplicated, inexpensive apparatus for orienting a relief map relative to light source so that topographic shadows can be photographed. The sundial method for model orientation (Aronin 1953, Olgyay and Olgyay 1957, Pleijel 1963) is used, but is modified to adjust for the vertical exaggeration found in many relief maps.

Standard sun machines might be used for illuminating undistorted maps. But they are not readily adapted for vertical exaggeration, and their non-parallel illumination is undesirable for accurate shadow projection.

Wise (1969a) contended that photographing shadows cast by plastic relief maps "seems to be among the more

remote of remote sensing techniques." Actually, we might think of it as a powerful analog computing method. Topographic information is stored in relief maps in a geometric analog format which is ideal for rapid shadow processing and retrieval merely by parallel illumination from the desired angle. Tens of thousands of intricate angles, distances, and elevations solve themselves instantly, as in the real landscape, creating shadow patterns without recourse to brute-force digital computation. The new technique represents utmost simplicity and efficiency.

A vast quantity of topographic information has been banked in this very functional form in plastic relief maps molded by the U.S. Army Map Service. These finely detailed maps cover most of the United States at 1:250,000 scale, and much of the rest of the world at various scales. These and other relief maps are now available from private manufacturers. If a plastic relief map for the area or at the scale desired cannot be obtained commercially, a relief model can be constructed from a standard topographic map sheet without much trouble. Hohausser (1970) and Taylor (1971) detail several simple, inexpensive methods for doing this.

#### Apparatus

Figure 2 illustrates the device developed for producing solar shadow maps from a plastic relief map.

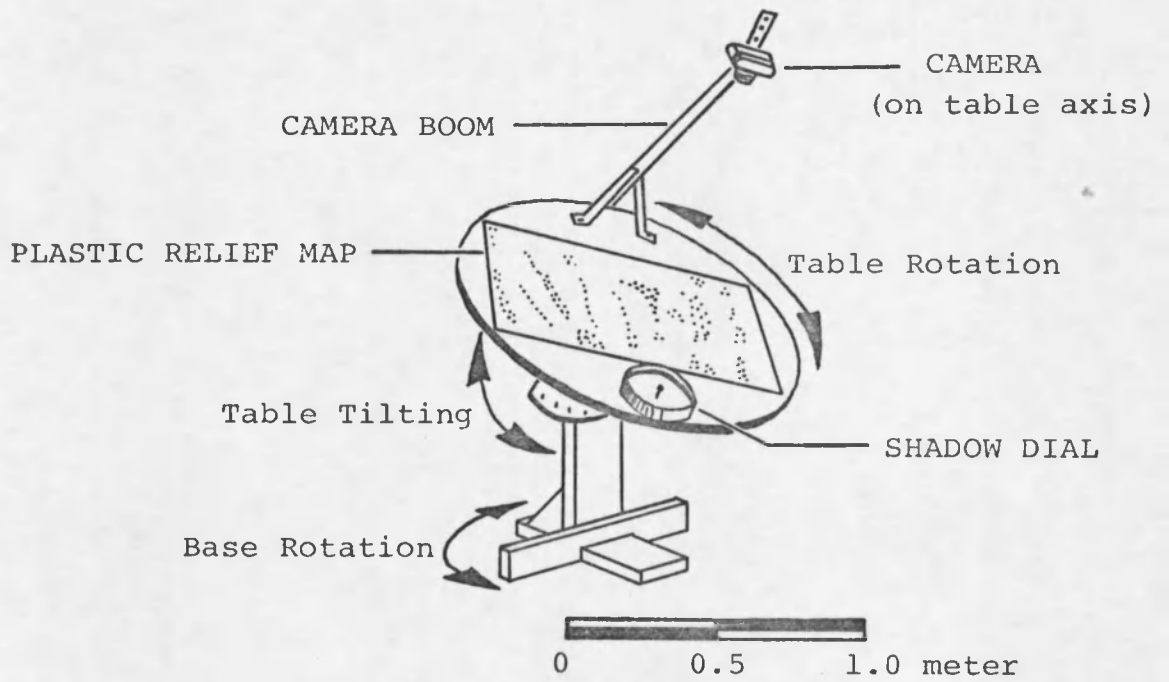


Figure 2. Solar shadow mapping apparatus

A round table with three degrees of rotational freedom permits orientation of the topographic model at any angle to the illumination source. Mounted on the table in precise directional alignment with the map is a sundial ("shadow dial") corrected for the appropriate vertical exaggeration (details in next section). A boom, also mounted on the table, holds a camera directly "over" the map area of interest, regardless of table tilt or rotation. The effect is that of aerial or orbital photography from model zenith. During this investigation, direct sunlight was used for model illumination. Any other nearly parallel light source will also work, however. The apparatus was built for less than \$20, excluding time, camera, and map.

#### Shadow Dial Geometry

Vertical exaggeration of a three-dimensional object only affects the vertical component of distances and angles. Thus, for relief models, azimuths and map distances are constant, but vertical distances (and hence the tangents of elevation angles) increase by the exaggeration factor. A sundial or shadow dial is essentially an angle meter, so the appropriate correction formula is:

$$\tan E_v = X \cdot \tan E$$

where X is the vertical exaggeration factor,  $E_v$  is the exaggerated elevation angle, and E is the original angle.

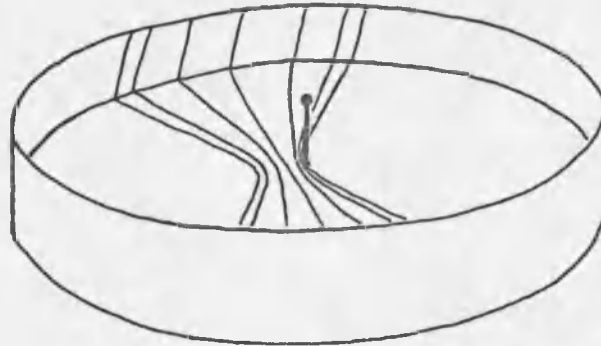


Figure 3. Shadow dial, perspective view  
Dial corrected for 2X vertical exaggeration.

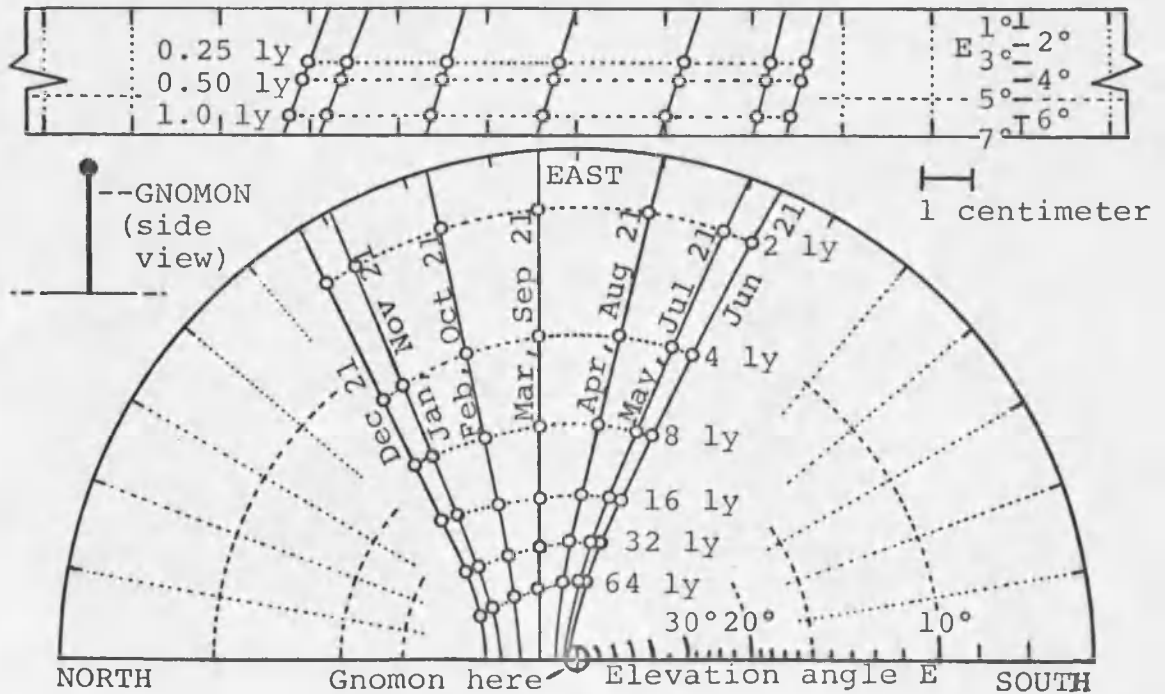


Figure 4. Shadow dial pattern for Mohawk Mountains study

Latitude 32° N. Vertical exaggeration 2X. Energy values in langleys (ly); significance discussed in text. Only half of dial is shown. Other half is mirror image.

A cylindrical shadow dial configuration (Figure 3) was developed to make vertical exaggeration calibration as easy as possible. This design is similar to but geometrically much simpler than Pleijel's square sundial with sloping sides (Aronin 1953, Olgyay and Olgyay 1957, Pleijel 1963).

Modeled sun position is read on the dial by noting the position of the gnomon shadow on a grid of radial equal-azimuth lines (unaffected by vertical exaggeration) and concentric-coaxial elevation angle circles (position adjusted by the formula given above). As shown in Figure 3, apparent daily sun paths for desired latitude and declinations can be plotted on this adjusted coordinate system. Figure 4 illustrates the actual shadow dial pattern and dimensions used in the Mohawk Mountains study (Chapter 4).

#### Procedure

Modeling shadows is easy and rapid. The relief map is mounted on the table in precise alignment with shadow dial north-south direction, with the area of interest centered beneath the camera. The table is then illuminated (usually by direct sunlight) and tilted and turned until the gnomon shadow is in correct position. A photograph is taken of the map shadows. Orientation and photography steps are repeated for each desired illumination angle. Later, the photo transparencies (usually black and white negatives) are

projected onto flat base maps and the shadow boundaries are traced. This raw shadow information can then be processed and analyzed in various ways.

### Discussion

Is this technique for topographic shadow mapping really new? A survey of the literature indicates that it probably is. Architects have been using similar illumination methods for a long time, and the shadows cast by topographic contours (which frequently are part of structure models) have surely been noticed on occasion. But attention has apparently been focused on the structures themselves; a vague reference by Aronin (1953) is the only architectural mention found of shade cast by illuminated model topography. And although photographs of relief maps showing distinct shadows have appeared in numerous places [Lee (1964), for instance], it seems that solar shadow maps have not been made from them until now. Finally, it is fairly certain that the apparatus developed for orienting and photographing relief maps, and the method for vertical exaggeration adjustment of sundial design are presented for the first time in this paper.

This new solar shadow mapping method offers a simple, rapid, inexpensive alternative to its closest competitors, the digital computer techniques. It may be more attractive than they when a raised-relief map of the

desired area at a suitable scale and accuracy is available commercially or can be constructed at low enough cost. It will be still more practical when computer time is unavailable or too costly, and when programming and topography digitization costs are too high. This new method is an elegant intermediate-technology tool which can model topographic shadows instantaneously and produce topographic shadow maps in minutes.

#### Alternative Uses

As noted in Chapter 2, Wise (1969a, 1969b) showed that photographs of illuminated relief maps can simulate side-looking radar (SLAR) images. With parallel illumination from simulated sun angles, low sun angle photography (LSAP) can be simulated even more accurately than SLAR. Such images could be used to choose optimum dates and times for actual LSAP flights, when surface shapes of interest (e.g. fault scarps) would be most sharply enhanced visually by low-angle solar illumination.

Shadows cast by objects other than topography and buildings could be mapped using the same apparatus. Such objects might include shrubs (Hinds and Richard 1968), trees (Aronin 1953), or clouds. The only prerequisites are a scale model of the object, and a suitably calibrated shadow dial.

Looked at in a different way, a solar shadow map is also a line-of-sight map. The sun can be seen from points outside umbra and shadow. Similar line-of-sight or shadow maps can be made, using the same apparatus, for any body far away enough to send approximately parallel light (artificial satellites, the moon, planets, stars).

Traditional line-of-sight studies have dealt with sets of points on or near the surface, however. Methods used for line-of-sight mapping have ranged from topographic profiling [similar to Garnett's (1935) technique (Lee 1964)], to elaborate computer programs (e.g., Snell 1961).

My philosophy in this paper is that three-dimensional geometric problems are often easiest to solve using a three-dimensional scale model. Line-of-sight maps can be prepared as fast as shadow maps by placing a tiny light source at the desired point on or above a raised-relief topographic map. Illuminated areas can be seen from (and can see) the reference point, while shaded areas cannot.

## CHAPTER 4

### MOHAWK MOUNTAINS STUDY

#### Introduction

Solar shadow maps were made of the northern part of the Mohawk Mountains, Yuma County, Arizona. The study was undertaken to perfect the new topographic shadow mapping technique and to demonstrate its effectiveness and practicality.

The Mohawk Mountains are a strikingly linear northwest-trending range in an extremely arid portion of the Sonoran Desert, in southwestern Arizona (see Figure 5). This range has a well-defined, long, sharp, jagged ridgeline crest, and its steep slopes are almost barren of vegetation. Peaks in the study area are commonly over 610 meters (2000 feet) above sea level, and over about 460 meters (1500 feet) above the surrounding plains. Dissected pediment (with a number of inselbergs) borders the range on both sides, and the broad alluvial piedmont surfaces beyond have very gentle slopes. A sand dune field parallels the range to the west. Interstate Highway 8 and the Southern Pacific Railroad slice through these mountains at a prominent pass. The geology of the area has been described by Bryan (1922, 1925), Darton (1933), Wilson (1933), and Babcock, Brown, and Hem (1947).

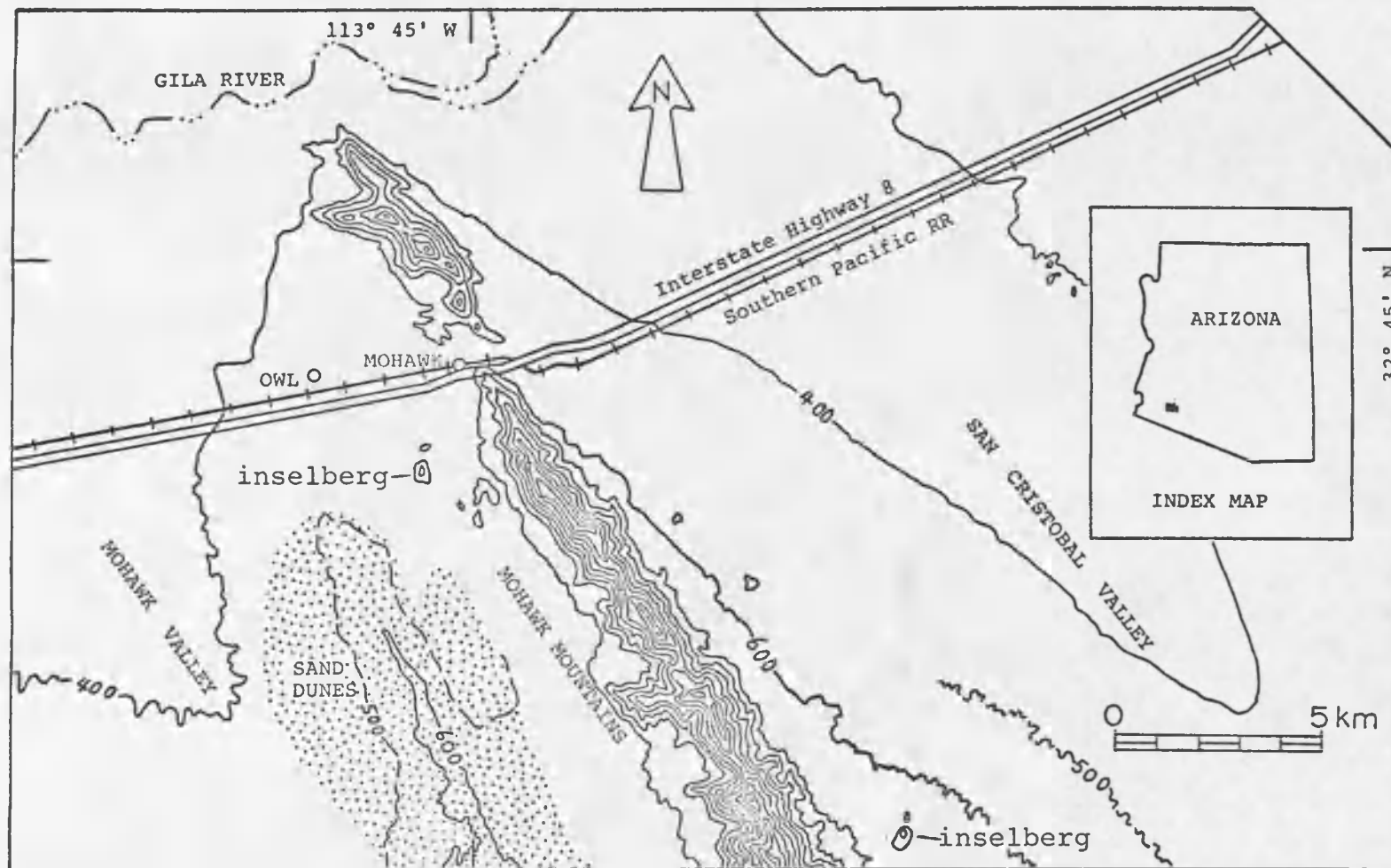


Figure 5. Mohawk Mountains topographic map

Contour interval 200 feet (61 meters) with supplemental contour at 100 feet (30.5 meters). Modified from U.S. Army Map Service (1960).

The Mohawk range was chosen for shadow mapping because:

1. It has almost unique geometric simplicity (single ridge with steep slopes). This results in fairly simple shadow patterns.
2. It is surrounded by relatively smooth, nearly horizontal piedmont areas. This also helps make shadow patterns simple.
3. It has a few small inselbergs nearby. As a result, the complexities of overlapping shadows can be demonstrated, but without making the shadow maps too confusing.
4. It is in an extremely arid region with a high percentage of clear days. This ensures that the shadow patterns have added significance.

Shadows were modeled using the procedure outlined in Chapter 3. The plastic relief map used was the 1:250,000 "Ajo, Arizona" quadrangle map (with 2X vertical exaggeration) originally produced by the U.S. Army Map Service (1960). A flat, paper version of the same map was enlarged for use as a base map.

#### Shadow Calibration Units

The shadow dial for this study was corrected for the 2X vertical exaggeration. Sun paths were plotted on it for monthly declinations at 32° north latitude (Figure 4).

Elevation angles for each month were determined to represent 1/4, 1/2, 1, 2, 4, 8, 16, 32, and 64 langleys of direct solar radiation on a horizontal surface cumulatively blocked daily either after sunrise (AM shadows) or before sunset (PM shadows). One langley equals one calorie per square centimeter ( $1 \text{ ly} = 1 \text{ cal/cm}^2$ ). Elevation angles were determined (Appendix B) for these values from a clear-sky solar radiation model (Appendix A) based on solar radiation records for Tucson, Arizona.

This geometric series of cumulative values was chosen in order to separate sequential shadow boundaries enough to avoid crowded shadow maps. The lowest value represents sun elevation angles just large enough ( $3^\circ$ ) not to be overly affected by warps in the plastic relief map. The highest value represents sun angles ( $31^\circ$  to  $38^\circ$ ) which shade mountain slopes but cast little or no projected shade onto the adjacent piedmont.

Shadows were calibrated, according to this series, in terms of cumulative energy on a horizontal surface in order to avoid the complexity of slope insolation. Also, most solar radiation records are for a horizontal instrument surface. Cumulative solar energy was used for calibration because it correlates directly with significant environmental variables like cumulative evaporation and cumulative heat absorbed. The shadows could just as easily have been

calibrated in units of instantaneous solar radiation rate, apparent solar time, or some other such variable.

Shadows in the mountainous parts of the study area were not mapped because their patterns would be too finely detailed for display at this scale. Shadows on the piedmont, which are shown in Figures 6 through 13, consist mostly (but not entirely) of projected shade. Morning shadows are projected to the west, afternoon shadows to the east. Shadows increase in cumulative energy value as they approach the mountains. Each cumulative energy value applies only to points on its respective shadow boundary line. Points within the boundary are shaded more; those outside are shaded less.

#### Accuracy and Error

Error and distortion can accumulate in several steps of the shadow mapping procedure. These steps include: molding, manufacture, and storage of relief maps; shadow dial construction; model mounting and orientation; shadow photography; photo projection; transfer of shadow data onto base map; and drafting of final map. Of these, only error involved in shadow dial construction and model orientation can be estimated with confidence: cumulative angle error within one degree. Information about relief map manufacturing tolerances is a key factor, but despite repeated requests to the manufacturer, none was supplied.

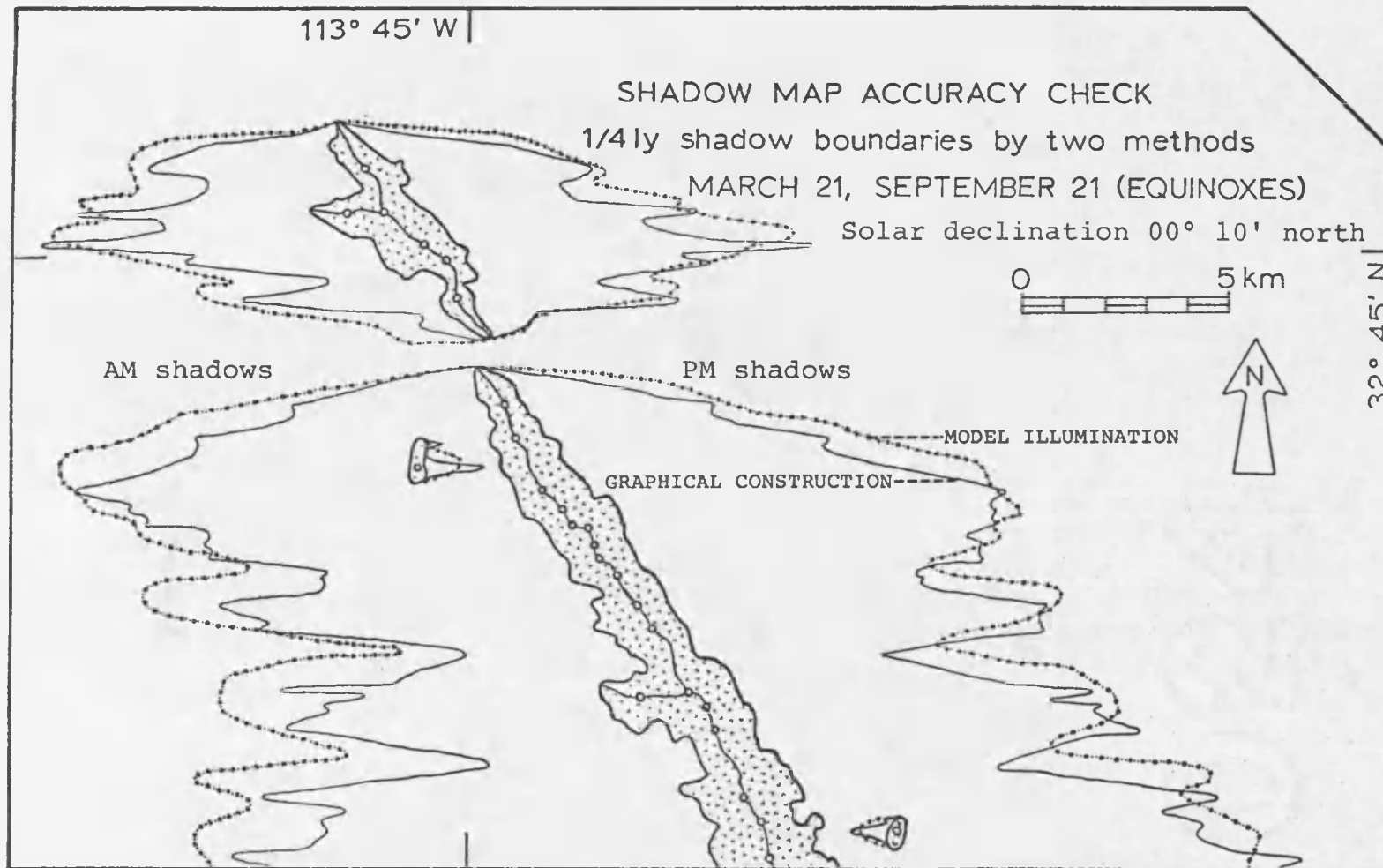


Figure 6. Mohawk Mountains shadow map accuracy check

Stippled area in this and following figures is mountainous region with steep slopes. Ridgelines and major peaks along them are indicated.

However, although detailed error analysis is not possible now, some idea of shadow map accuracy is conveyed by Figure 6. This illustration shows shadow boundaries for 1/4 ly cumulative energy blocked at the equinoxes, determined by two methods: relief model illumination, and precise but extremely time-consuming graphical construction from a topographic map [technique modified from that of Garnett (1935)].

These two methods produce notably similar results. The plastic model obviously generalizes the topography to an extent, and major peaks and saddles are slightly displaced. But the model is remarkably precise and detailed, considering that its actual size is approximately 2/3 that of the figure reproduced here. Systematic discrepancy between AM shadow lengths in Figure 6 is probably due to slight model orientation error. It can be seen, then, that shadow maps produced from plastic relief models do provide a good approximation of the real shadows.

#### Sample Shadow Maps

In Figure 7, sequential shadow boundaries are combined in one shadow map for summer solstice (June 21). Figures 8 through 13 are similar maps of shadow patterns at monthly intervals, including the equinoxes (Figure 10) and winter solstice (Figure 13). In all these maps, the outermost shadow boundary corresponds to 1/4 ly of direct

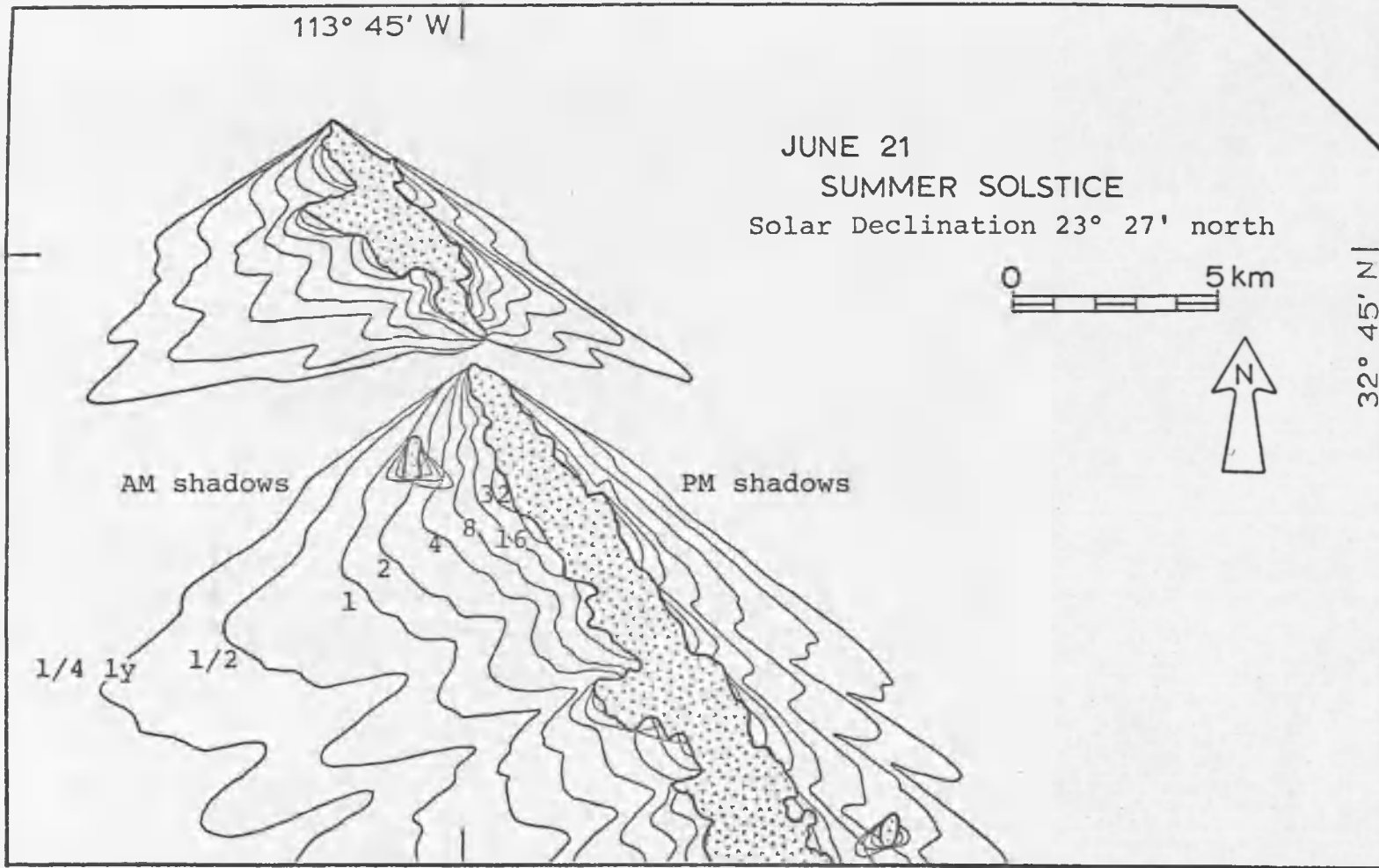


Figure 7. Mohawk Mountains shadow map: June 21 (summer solstice)

Units and magnitudes represented by shadow boundaries in Figures 6 through 14 are explained in the text (fourth subsection of Chapter 4).

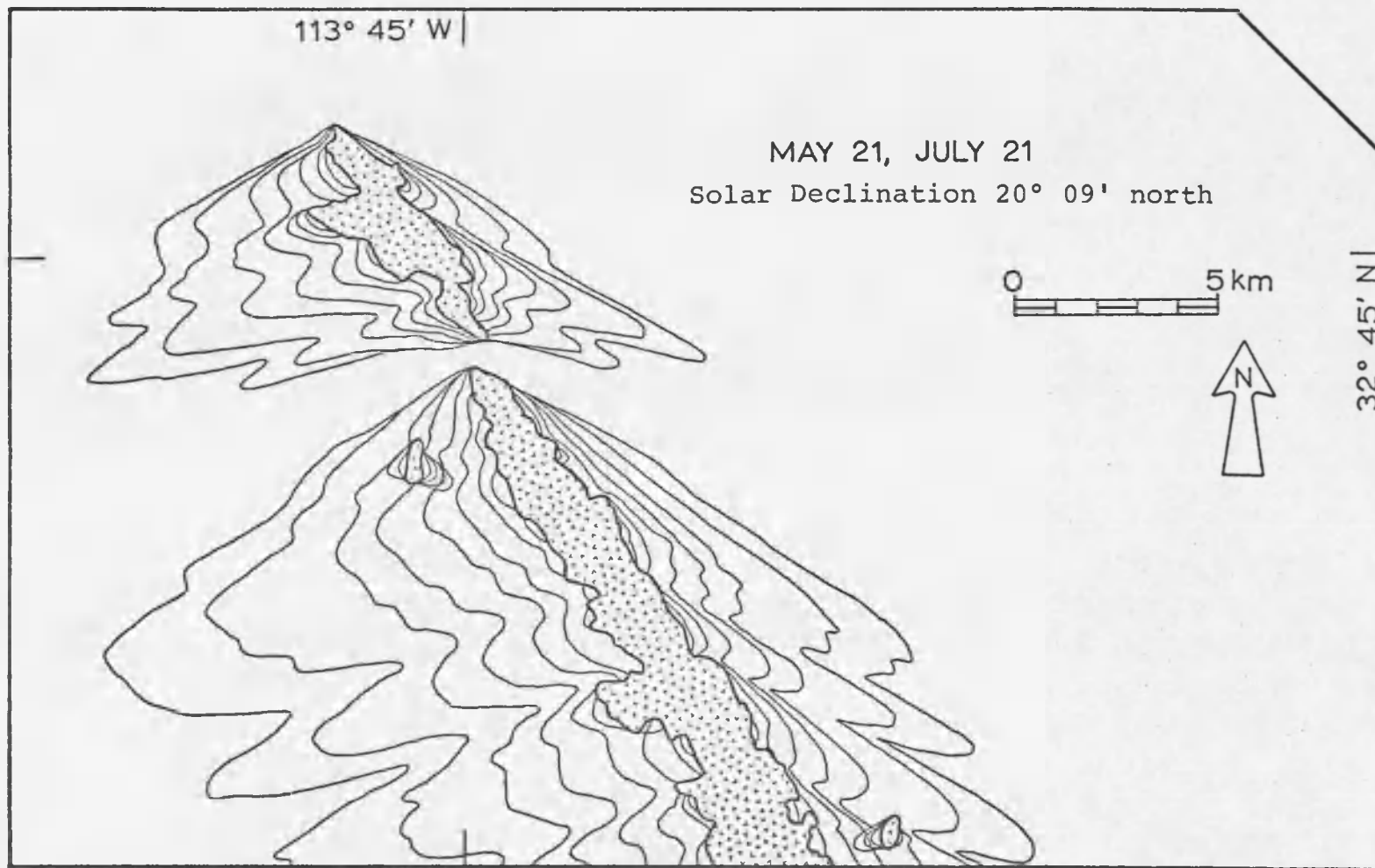


Figure 8. Mohawk Mountains shadow map: May 21, July 21

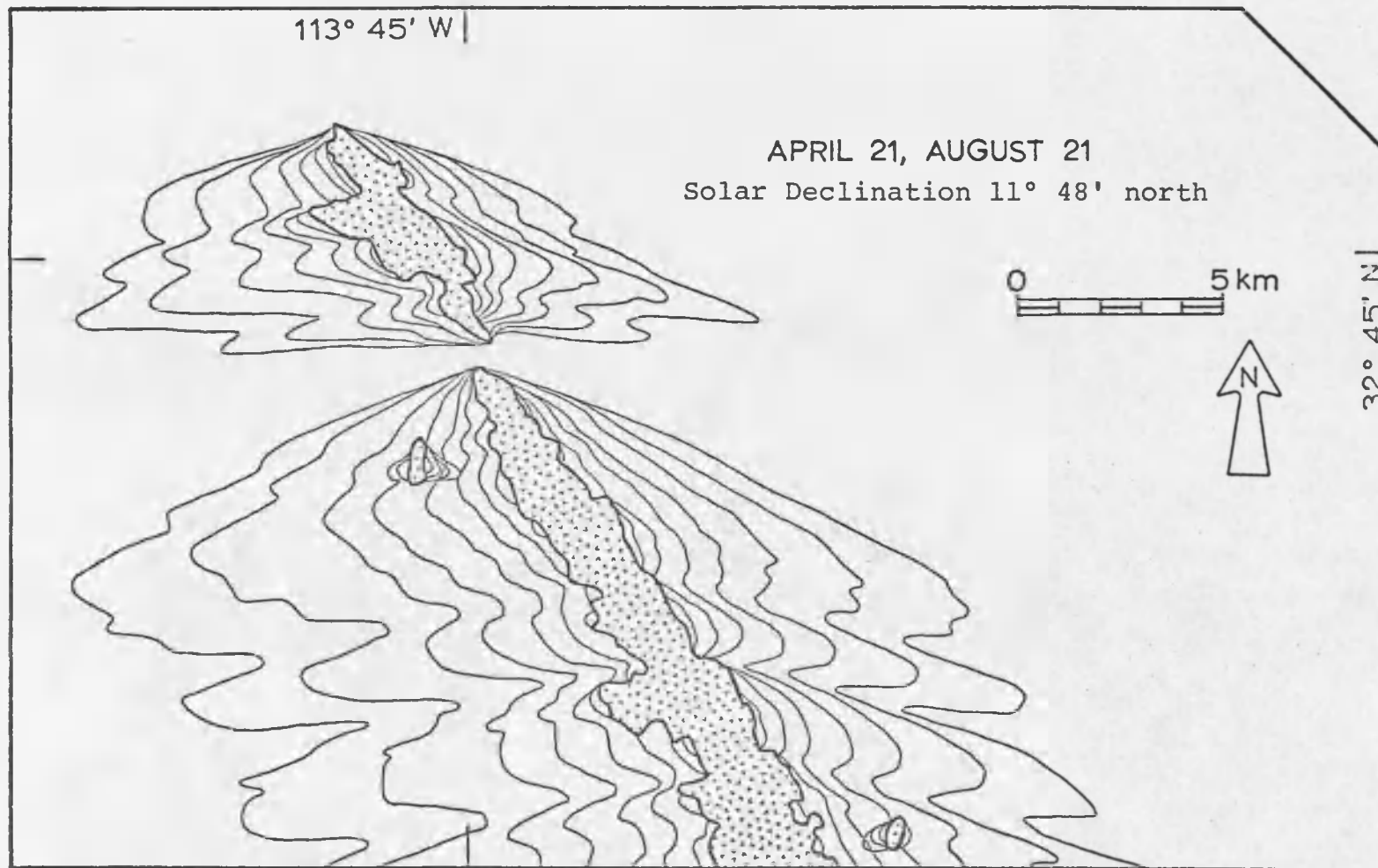


Figure 9. Mohawk Mountains shadow map: April 21, August 21

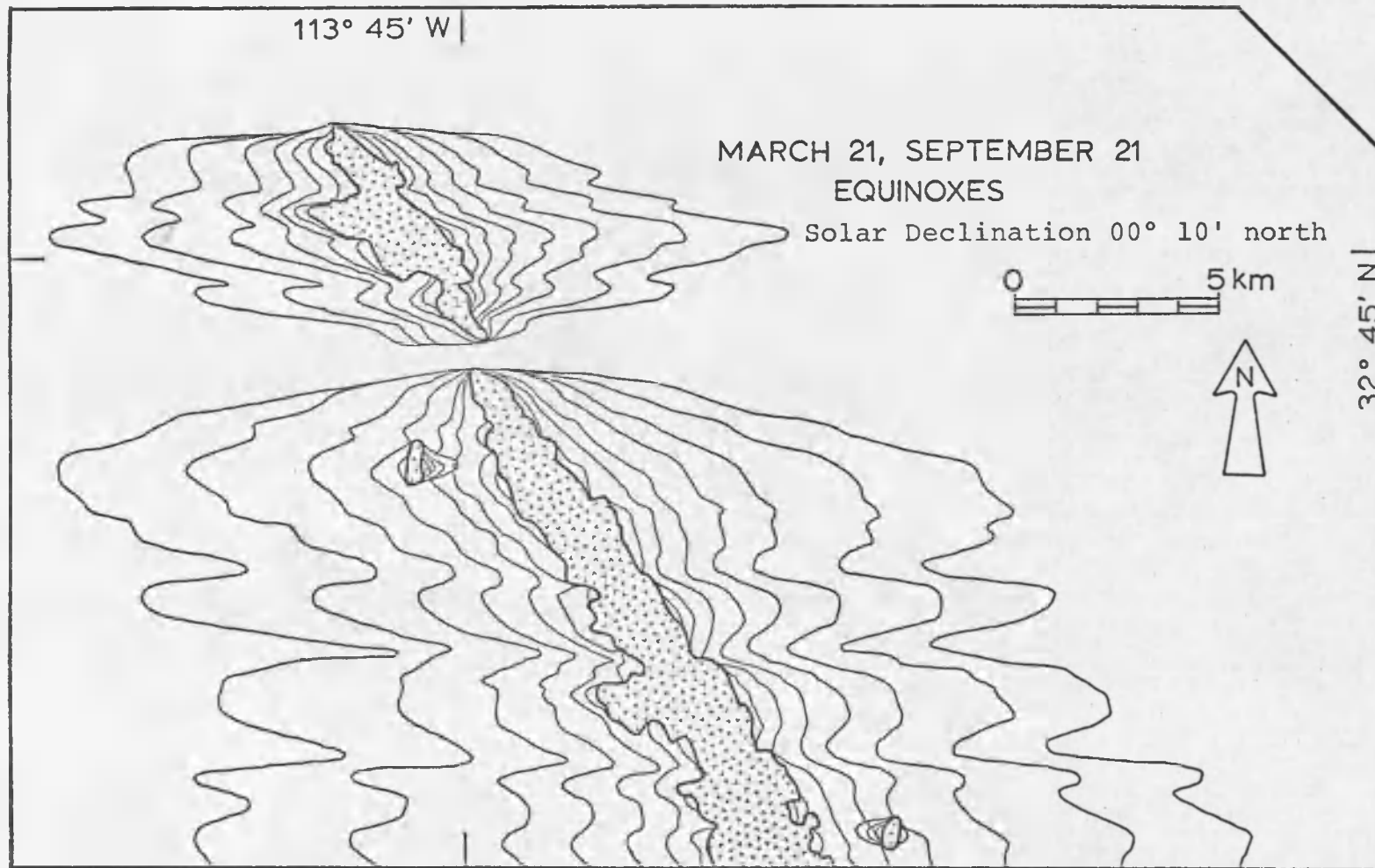


Figure 10. Mohawk Mountains shadow map: March 21, September 21 (equinoxes)

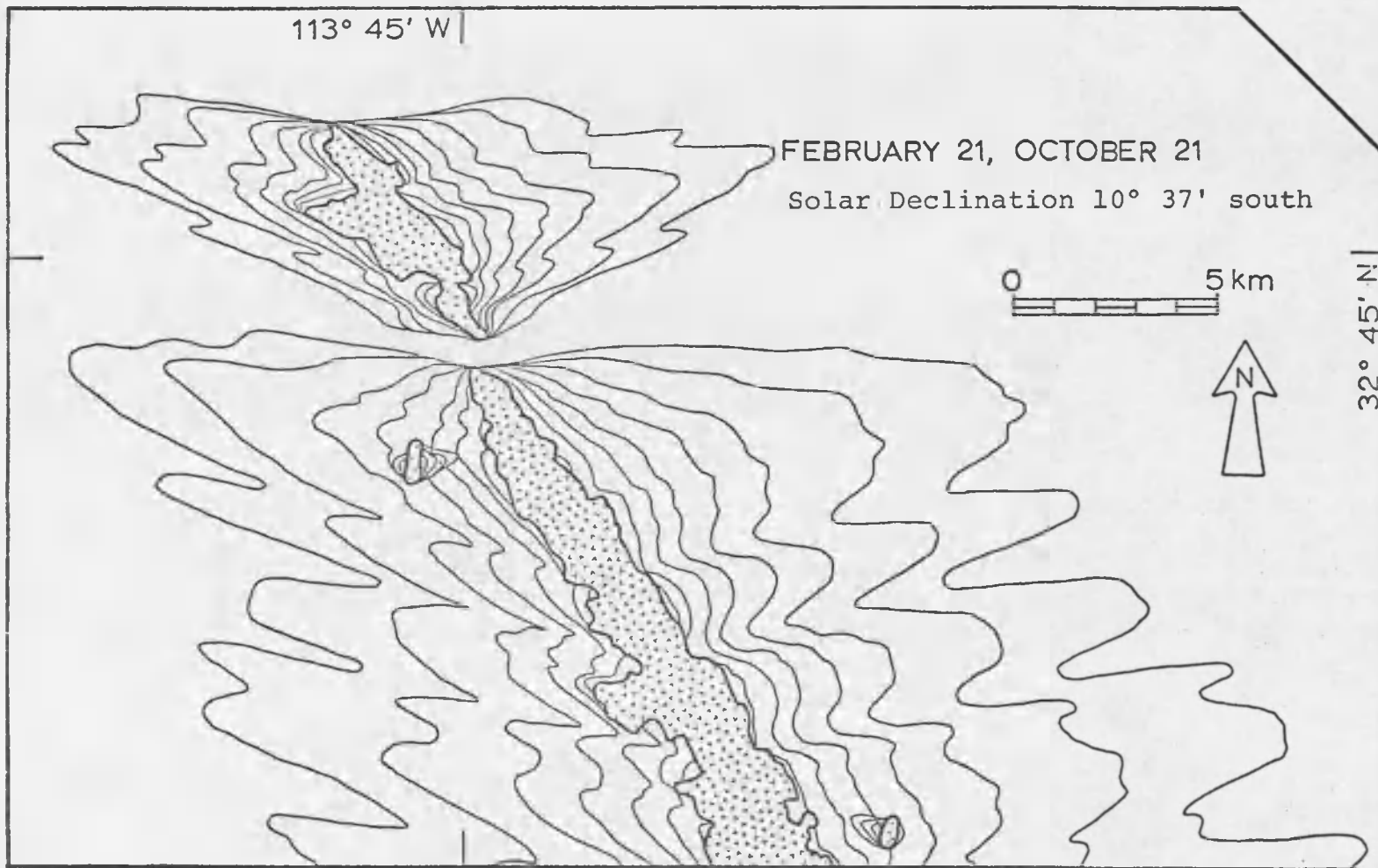


Figure 11. Mohawk Mountains shadow map: February 21, October 21

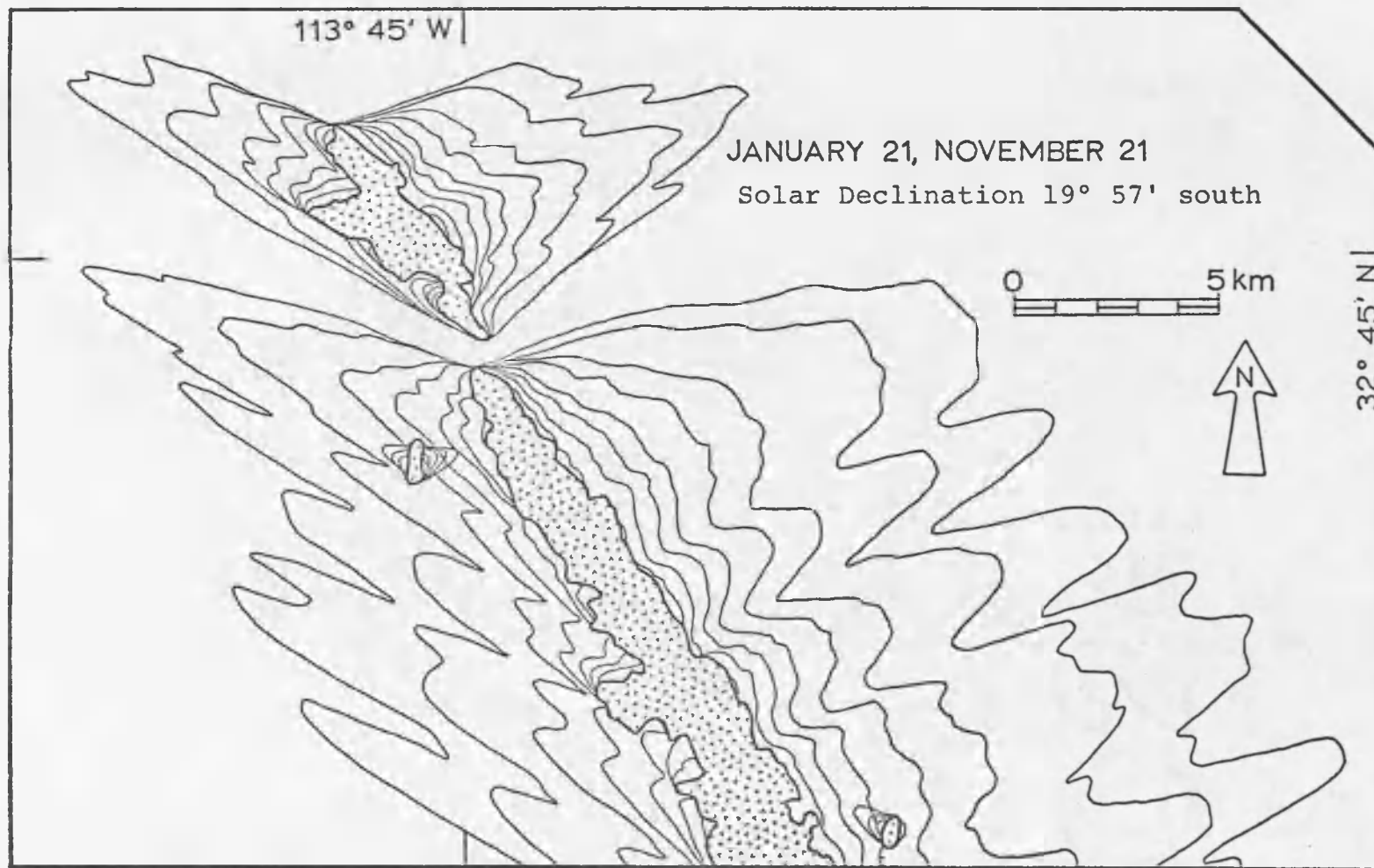


Figure 12. Mohawk Mountains shadow map: January 21, November 21

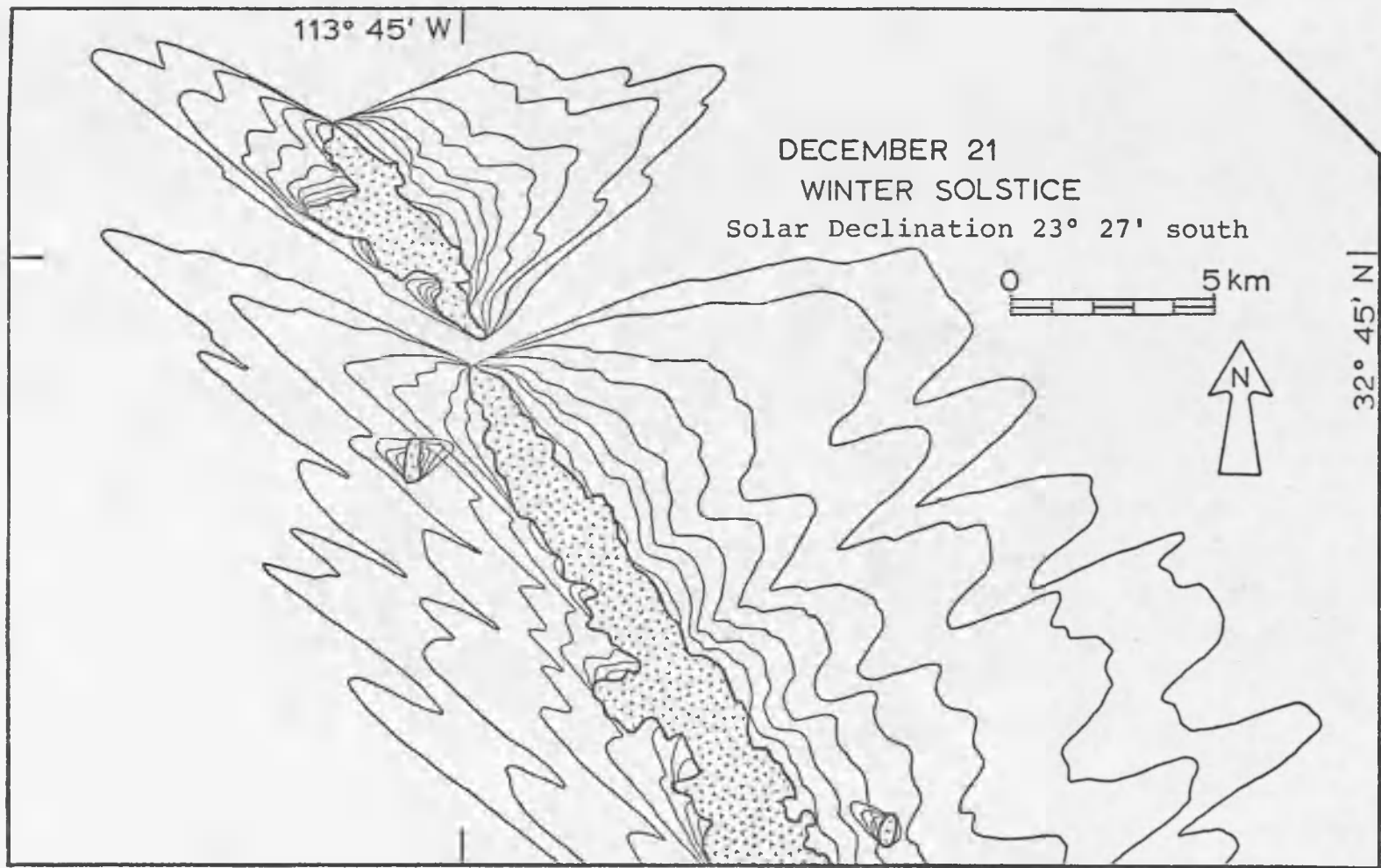


Figure 13. Mohawk Mountains shadow map: December 21 (winter solstice)

solar radiation on a horizontal surface cumulatively blocked daily either after sunrise (AM shadows) or before sunset (PM shadows). Boundaries progressively closer to the mountains (or inselbergs) represent 1/2 ly, 1 ly, 2 ly, 4 ly, and so forth. AM shadows are to the west; PM shadows are to the east. With maps like these the Mohawk Mountains are converted to a giant calibrated sundial.

Comparison of Figures 7 through 13 reveals a dramatic seasonal change in relative areas of AM and PM shadows. This is a direct result of mountain range orientation oblique to the cardinal directions. Shadow areas are largest (for specific elevation angle) when illumination is perpendicular to range trend.

Two inselbergs in the study area complicate the shadow patterns slightly. AM shadow boundaries of the eastern inselberg overlap PM shadows cast by the main range, and just the opposite occurs for the western inselberg. For points in the overlap zones, the effect is additive; these points are shaded both morning and afternoon.

Figure 14 is a map of annual envelopes which enclose individual shadow boundaries of equal value as they sweep north and south through the year. This is just one of many possible ways to synthesize and process the raw shadow data.

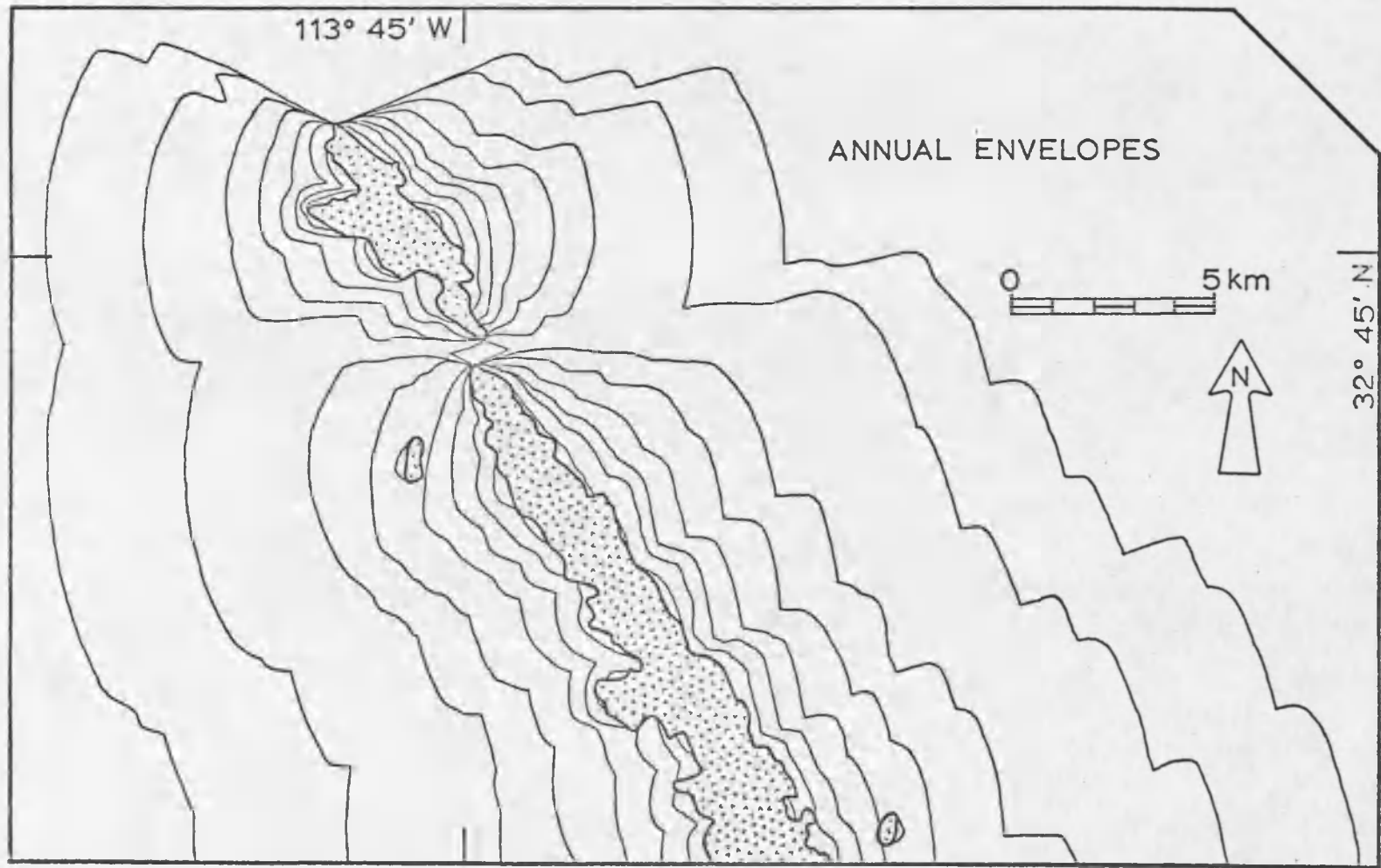


Figure 14. Mohawk Mountains shadow map: annual envelopes

### Shadow Implications

What is the effect of these shadows mapped for the Mohawk Mountains area? Aside from instantaneous illumination differences, the cumulative effect is probably rather small in most of the shaded area. This is because the highest value piedmont shading reaches is 32 ly, which is a mere 5 to 13 percent of total direct insolation on an unshaded horizontal surface (246 to 692 ly, from Appendix B). And only small areas near the mountain-piedmont junction are shaded as much as 8 ly (1 to 3 percent of daily direct insolation). The effect of shade would be larger, but still minor, on slopes facing the mountains. Probably only shadows within the rugged mountainous area itself (not mapped in this study) would have a noticeable cumulative effect on such variables as evaporation and vegetation cover.

However, these shadows on the piedmont seem more impressive when the large total energy loss they represent is calculated. For example, as determined in Appendix C, the piedmont shadow areas in Figure 7 represent a total daily energy loss of  $87 \times 10^{10}$  calories (1020 megawatt-hours), equivalent to 42.5 megawatts of continuous power (the output of a medium-size power plant).

Furthermore, it is fascinating to realize that these same ephemeral shadow patterns have recurred with clockwork

regularity year after year for a large span of history. If we assume a denudation rate of 5 centimeters per thousand years (William B. Bull, Professor of Geosciences, University of Arizona, personal communication, October, 1975), then the Mohawk Mountains shadow patterns have not changed significantly in 500,000 years.

## CHAPTER 5

### APPLICATIONS

#### Preview

Now that this new technique has been developed, topographic shadow mapping may be practical for many studies that were unfeasible before. A brief suggestion of such possible applications seems appropriate here.

As pointed out in the introduction, shade affects the whole galaxy of phenomena and variables which solar radiation influences. Some effects are direct; many involve feedback or long chains of causality and interaction. Topographic shading is especially significant where the atmosphere is clear (arid and semiarid lands, alpine regions) or absent (the moon), where slopes are steep (mountains, craters, escarpments), in middle and high latitudes, and in winter (low sun angles).

References to shade-related solar radiation work are scattered widely through the literature of numerous disciplines. Perhaps this chapter, in addition to suggesting shadow map applications, will be useful by itself as a compendium of diverse solar-affected phenomena, and a quick stepping-stone to the massive applied solar radiation literature.

Phenomena that might be studied using solar shadow maps are listed here under five system categories: microclimatic systems, hydrologic systems, geological systems, biological systems, and human and industrial systems.

### Microclimatic Systems

Microclimatology [or topoclimatology (Thorntwaite 1954)] is the most abstract and universal approach to study of local solar radiation and shadow effects. Solar radiation and its absence profoundly influence the many earth-air energy and matter exchange mechanisms (Sellers 1965; Geiger 1965, 1969).

Surface temperature rise is the most obvious solar radiation effect (Shreve 1931, Rouse and Wilson 1969). When atmosphere is clear or absent, thermal contrast across shadow boundaries is most extreme. Solar radiation also supplies energy for increased water evaporation from surfaces (Shreve 1931, Abd el Rahman and Batanouny 1966, Martsolf 1966, and Hellwig 1973), directly affecting potential evapotranspiration (Nash 1963, Lee 1964). Thus sun and shade directly influence surface energy balance (heat budget, radiation balance, net radiation) and surface water balance (Lee 1964, Rouse and Wilson 1969, Wilson 1970).

Air temperature and humidity vary with surface heating and evaporation (Shreve 1931, Martsolf 1966, Rouse and Wilson 1969, Hellwig 1973). And local air differences result in slope convection, air currents, and wind velocity changes (Geiger 1965, Abd el Rahman and Batanouny 1966). Finally, shade and sunlight largely determine visible illumination levels--the illumination climate (Reitan and Green 1968).

#### Hydrologic Systems

Sunlight speeds evaporation from soil and rock surfaces (Martsolf 1966, Hellwig 1973), thus affecting water balance (Nash 1963, Lee 1964, Rouse and Wilson 1969, Wilson 1970), soil moisture (Wilson 1970, Reid 1973), and surface runoff (Reid 1973). Solar soil heating influences freeze-thaw timing (Sartz 1972, Koutz and Slaughter 1973), and permafrost presence or absence and thaw depth (Koutz and Slaughter 1973, Dingman and Koutz 1974).

Snowmelt is accelerated by sunlight, retarded by shade, with effects on water balance, soil moisture, and runoff (Garnett 1935, Anderson and West 1965, Garn 1969, Rouse and Wilson 1969, Koutz and Slaughter 1973). Topographic diversity of watersheds (variable slope orientation and steepness) results in time and space variations of snowmelt rate, thus delaying and smoothing runoff peaks--a natural flood control mechanism (Hendrick, Filgate, and Adams 1971;

Sartz 1972). (This is analogous to increased stability of biological ecosystems with greater diversity.)

Shade- and sun-influenced snowmelt rate also determines whether glaciers advance, retreat, or exist at all in specific locations (Lougeay 1970, Andrews 1971, Williams, Barry, and Andrews 1972). The retarding effect of topographic shade on melt of snowpacks and glaciers may, however, be counteracted by sunlight reflected from nearby high albedo slopes (Anderson and West 1965, Andrews 1971).

Solar radiation also raises the temperature of surface water bodies such as streams, ponds, lakes, and tidal pools (Horton 1966, Brown 1970, Meehan 1970, Calandro 1973), and provides energy for evaporation from them. Topographic shade retards evaporation and conserves water, for instance in rock tanks (tinajas) of desert regions (Bryan 1925, Ives 1962). Shading by phreatophytes along a desert stream may actually reduce evaporation more than the amount lost through transpiration (Horton 1966).

### Geological Systems

Sunlight and shade play essential roles in many surface-geological and geomorphic processes. For example, solar radiation intensity and its fluctuations affect mechanical weathering of rocks either directly (insolation weathering) or indirectly (freeze-thaw disintegration) (Ollier 1969). In deserts, chemical weathering is enhanced

by shade because it slows evaporation of moisture in pore space (Peel 1960, Roth 1965). This suggests a possible feedback mechanism in cavernous weathering: shading by overhang speeds weathering below it.

Soil moisture content, which varies with sunlight, influences soil chemistry, soil formation rate, soil structure (thus also porosity and infiltration rate), and soil depth (Reid 1973). We might expect slope insolation and topographic shade to partly determine depth of caliche in soils of arid lands. Soil temperature, increased by insolation, may also affect pedogenesis rate, as well as freeze-thaw and permafrost presence and depth (Soons and Rainer 1968).

Slope variables indirectly affected by sun include erosion rate, drainage density, and soil movement rate (creep or mudflow), which are influenced by freeze-thaw or soil moisture (Soons and Rainer 1968, Reid 1973). These variables, in turn, help determine slope steepness (Melton 1960), sediment yield, and runoff, which in turn affect stream hydrology and morphology, downcutting, and sedimentation phenomena. Glaciers in marginal locations may perpetuate themselves by topographic shade from the steep-walled cirques which they gouge out. Shaded slopes of dunes may be the first areas to be stabilized by vegetation.

## Biological Systems

Sunlight and shade affect biological systems not only directly, but also indirectly through influence on microclimatic, hydrologic, and geological systems. Animal behavior is frequently adapted to sun and shadow effects, but plants are probably more sensitive to the many environmental factors which vary with solar radiation.

### Plant Physiology

Physiological parameters which react directly and rapidly to changes in ambient solar illumination level include: plant temperature--shade helps survival in heat, sun helps prevent freezing--(Martsolf 1966, Despain 1967, Hinds and Richard 1968, Gibbs and Patten 1970); transpiration rate and stomatal opening size (Shreve 1931, Abd el Rahman and Batanouny 1966, Martsolf 1966); respiration rate (Despain 1967); and photosynthesis rate--too much shade slows rate, but too much sun destroys chlorophyll-- (Despain 1967).

Some physiological functions and parameters which respond directly and indirectly to patterns of sunlight and shade over a period of time are: seed germination (Shreve 1931); seedling survival--of forest trees (Ronco 1970) and saguaro cactus (Despain 1967, Brum 1973)--; phenology (Brum 1973); growth and size (Shreve 1931, Rouse and Wilson 1969, Wilson 1970); tree ring thickness; and generalized plant

productivity--shade enhances it in arid climate where water is limiting factor, but diminishes it in humid climate where sun is limiting factor.

### Plant Geography and Ecology

Vegetation assemblage at a specific location consists of plants which best survive under local sunlight-influenced environmental conditions (Shreve 1931, Wilson 1970, Koutz and Slaughter 1973). This should be considered when attempting vegetation establishment (Fons, Bruce, and McMasters 1960; Tiedemann, Klemmedson, and Ogden 1971; Koutz and Slaughter 1973). Similarly, vegetation distribution and zoning at various scales in space may be determined in part by sunlight and shadow relationships (Shreve 1931, Abd el Rahman and Batanouny 1966, Dingman and Koutz 1974).

Some plants and animals depend on shade caused by other plant species. For example, saguaro seedlings survive better under palo verde shade (Despain 1967). Thus plant shade, by increasing small-scale environmental diversity, expands the number of plant and animal species which can coexist in an area (Hinds and Richard 1968).

### Cultivated Plants

Sunlight is an important parameter in forestry. It influences forest entomology, pathology, fire susceptibility and control, growth rate, and productivity (Fons, Bruce, and McMasters 1960; Ronco 1970; Wilson 1970; Buffo, Fritschen,

and Murphy 1972; Sartz 1972). In agriculture, solar radiation and shade affect water requirements, plant survival, productivity, optimal forest-pasture distribution in alpine areas, and timing of crop ripening (Garnett 1935). In "primitive" agriculture small-scale topographic shade might effectively reduce crop water needs. Shade and sun also help determine plant choice and location in landscape planting (Sacamano and Duffield 1971).

### Animals

Much animal behavior seems to be aimed at thermoregulation; dogs seek shade when hot, avoid it when cold. Similar behavior is reported for small mammals (Lowe and Hinds 1971) and beetles (Hamilton 1971). Despain (1967) describes an interesting plant-animal relationship in the Sonoran desert: animals collect saguaro fruits and seeds and take them to eat in the shade. Seeds dropped there have better chances for germination and seedling survival.

### Human and Industrial Systems

#### Aesthetics and Ritual

The aesthetics of solar illumination are pervasive in our lives. The shadows we map are a repetitive, long-lived aspect of the visual landscape. Shadow maps might be used to determine sunset visibility for a site.

Sun position, indicated by shadow angle, is important in the daily and annual rituals of many cultures. Examples are the probable prehistoric use of Stonehenge, and the precise seasonal ritual cycle of the Hopi Indians. The association of ritual with sun position often has good reason: sun path is closely correlated with seasonal rhythms in diverse climatic, hydrologic, and biological systems upon which a culture depends. Vestiges of sun-correlated rituals remain in our year-round 24-hour-a-day industrial civilization.

#### Archaeology, Architecture, and Urban Planning

Industrial systems (dwellings, settlements, agriculture, industries) are influenced in many ways by solar radiation angles and amounts. Formerly, solar energy (either direct or recently impounded) ran almost all human life-support systems. Now that we are using fossil fuel storages to power increasingly massive and complex systems, the solar cycles are not so all-determining. However, as fuel supplies dwindle, solar radiation patterns will regain their importance to industrial cultures.

Archaeology reveals the extent of the sun awareness of earlier peoples in their design of dwellings. Knowles (1974) analyzes the sophistication of the design (geometry and materials) and siting of pueblos and cliff dwellings in Southwestern U.S. In Tsegi Canyon, Arizona, all twelve

cliff dwellings are sited in caves which open south for natural microclimate control: the overhang shades in summer, but lets sunlight through in winter (Dean 1969). Clearly, solar shadow maps might be quite useful in future archaeological investigations of dwellings and agricultural sites in areas with steep slopes and escarpments.

Insolation amount is a significant factor in today's architecture as well as that of the past. If sunlight is not considered during design, much expensive air conditioning is necessary to offset it. However, there are many ingenious ways to take advantage of sunlight and shade in building design and siting (Aronin 1953, Pleijel 1954 and 1963, Olgay and Olgay 1957), and these are rapidly gaining popularity. On a larger scale, energy conservation calls for adoption of similar design strategies in urban planning (Aronin 1953, Pleijel 1954, Knowles 1974). Knowles (1974) envisions three-dimensional mega-structure cities designed with consideration for sun path geometry.

### Recreation

Sunlight plays an important part in many types of recreation. Not only is it vital for sunbathing on beaches (Puerto Rico Planning Board 1969), but it should also be considered in siting playgrounds and parks, especially at higher latitudes (Aronin 1953, Pleijel 1963). Sun and shade

also strongly influence the depth and quality of snow on ski runs (Hendrick, Filgate, and Adams 1971).

### Solar Technology

Solar illumination and shading must be considered in the design, layout, and siting of solar-powered devices and industries, including water and air heaters, power plants, stills, and evaporation ponds. In the aerospace industry shadows have been mapped for solar cell panels on satellites by both model illumination and computer techniques (Robert S. Sternberg, graduate student, University of Arizona, personal communication, April, 1975). Installing solar power plant collectors in abandoned open-pit copper mines has been proposed (Matter et al. 1974); shadow maps might help site these collectors within the pit.

Actually, this thesis started out as a study of landscape factors which might influence siting of solar power plants. Most previous siting work has focused on atmospheric conditions. But the terrain (including shadows it casts) will help determine specific sites within atmospherically favorable regions.

### Legal Aspects

As the importance of solar radiation to industrial systems becomes better known, we may expect the development of sun-and-shade litigation and legislation. Can one man build a structure in front of another's solar heater panels?

Shadow maps may have their days in court. The Puerto Rico Planning Board (1969) studied the problem of shading of beaches by high-rise hotels. Their consideration of zoning on the basis of shadow maps may be an indication of things to come.

### Industrial Ecology

Throughout history, human settlement patterns have been influenced by many environmental variables, including sunlight and shadow. Garnett (1935) shows that distribution of forest, pasture, farmland, and villages in the Alps, worked out through centuries of trial and error, has come to reflect solar radiation and shadow distribution. Knowles (1969, 1974) finds sun-influenced patterns in Indian activity locations in Owens Valley, California. Fuggle (1971) found that Basuto dwellings (in Lesotho) are usually sited on slopes facing early morning sun.

Since the Industrial Revolution there has been a rapid expansion of new, complexly interlocking industrial systems. By analogy to biological systems, which they look like from aloft, we can call them "industrial ecosystems". They have evolved and spread across the landscape through a series of many small individual decisions and actions. Frequently, habitual industrial patterns have been thrust into new environments for which they were not designed

(for instance, large glass windows in buildings of hot deserts), and have been sustained there only by use of heavy fossil fuel subsidies.

We can afford such subsidies less and less. Knowles (1974) points out that for survival, design diversity and location of industrial systems should reflect environmental diversity just as sensitively as biological systems do, thus taking advantage of naturally occurring matter and energy gradients and flows. Both Garnett (1935) and Knowles (1974) contend that it will be to our advantage to make such adjustments consciously, now that we know the natural patterns better, rather than unconsciously through inefficient, time-consuming trial and error (as in the past). Perhaps solar shadow maps will be one tool to assist us in our conscious industrial evolution.

## APPENDIX A

### SOLAR RADIATION MODEL FOR SOUTHERN ARIZONA ATMOSPHERE

If atmospheric properties are assumed to be constant and horizontally homogeneous, then direct normal-incidence solar radiation rate ( $Q_n$ ), and direct, diffuse, and total solar radiation rates on horizontal surface ( $Q$ ,  $q$ , and  $Q+q$ ) are functions of solar elevation angle ( $E$ ), only. Although these functions do not vary for a specific atmospheric state, they do depend complexly on such atmospheric variables as transmissivity, pressure, and water vapor content. Numerous authors have tabulated typical values of solar radiation rates for varying  $E$  (e.g., Reifsnyder and Lull 1965), and others have presented quantitative techniques for estimating values based on assumptions about atmospheric conditions (e.g., Fons, Bruce, and McMasters 1960; Robinson 1966).

However, for the Mohawk Mountains study (Chapter 4) it seemed desirable to develop an empirical solar radiation model based on atmospheric conditions typical of clear days in southern Arizona. The model is based on solar radiation data recorded on July 10, 1974 at the observation station of the Institute of Atmospheric Physics, University of Arizona, Tucson, Arizona.

This appendix outlines the steps taken to process the data and determine typical functions of solar radiation parameters with respect to solar elevation angle  $E$ . These relationships, in turn, have been used (Appendix B) to construct solar radiation versus time curves for representative days of the year. And these curves have been used to calibrate shadow dial and shadow maps in the Mohawk Mountains study.

The records for July 10, 1974 were chosen as the basis of the model for several reasons: (1) July 10 was a very clear, almost cloud-free day. (2) It was near summer solstice, so the sun approached the maximum annual solar elevation angle at solar noon. (3) The instrument records are good and nearly complete for that day. (4) Other experiments (sky radiance mapping, not included in this thesis) were done that day. And (5) the apparent atmospheric transmission index for  $Q+q$  data was 0.776, very close to the annual average of about 0.765 (determined from a systematic sample of 84 clear days from July, 1973 through June, 1974). Apparent atmospheric transmission index is the ratio of  $Q+q$  at noon to total solar radiation at the top of the atmosphere, and is recorded for each clear day.

Solar radiation data are recorded with respect to time, whereas the relationship to  $E$  is needed for the general model. To make this conversion without computer, solar elevation angle  $E$  as a function of time (hour angle  $T$ )

is accurately and rapidly determined from latitude L and declination D using a graphical technique (Robinson 1966, p. 148-149) based on the formula

$$\sin E = \sin D \cdot \sin L + \cos D \cdot \cos L \cdot \cos T.$$

For a given location and date, D and L are constant, and sin E is a linear function of cos T. This function is easily plotted, on a graph with sin E and cos T axes, as a straight line connecting points calculated for cos T = 0 and cos T = 1. Figure 15 is such a graph for Tucson on July 10. Data from this figure for 10-minute intervals are listed in Table 1, column B.

Raw data for  $Q_n$  and  $Q+q$  at 10-minute intervals (Table 1, columns C and F) were multiplied by instrument calibration factors and plotted versus time (Figure 16). Curves fitting these points yielded smoothed  $Q_n$  and  $Q+q$  data (Table 1, columns D and G), which were used to calculate Q and q values (Table 1, columns E and H, and Figure 16).

Finally, in Figure 17, the four solar radiation parameters are plotted with respect to solar elevation angle E. In this way the model is generalized by removing the effects of latitude and declination. These curves make possible prediction of instantaneous solar radiation rates as long as E is known and similar atmospheric conditions are assumed. Solar radiation values for selected E values (from Figure 17) are listed in Table 2 for convenient reference.

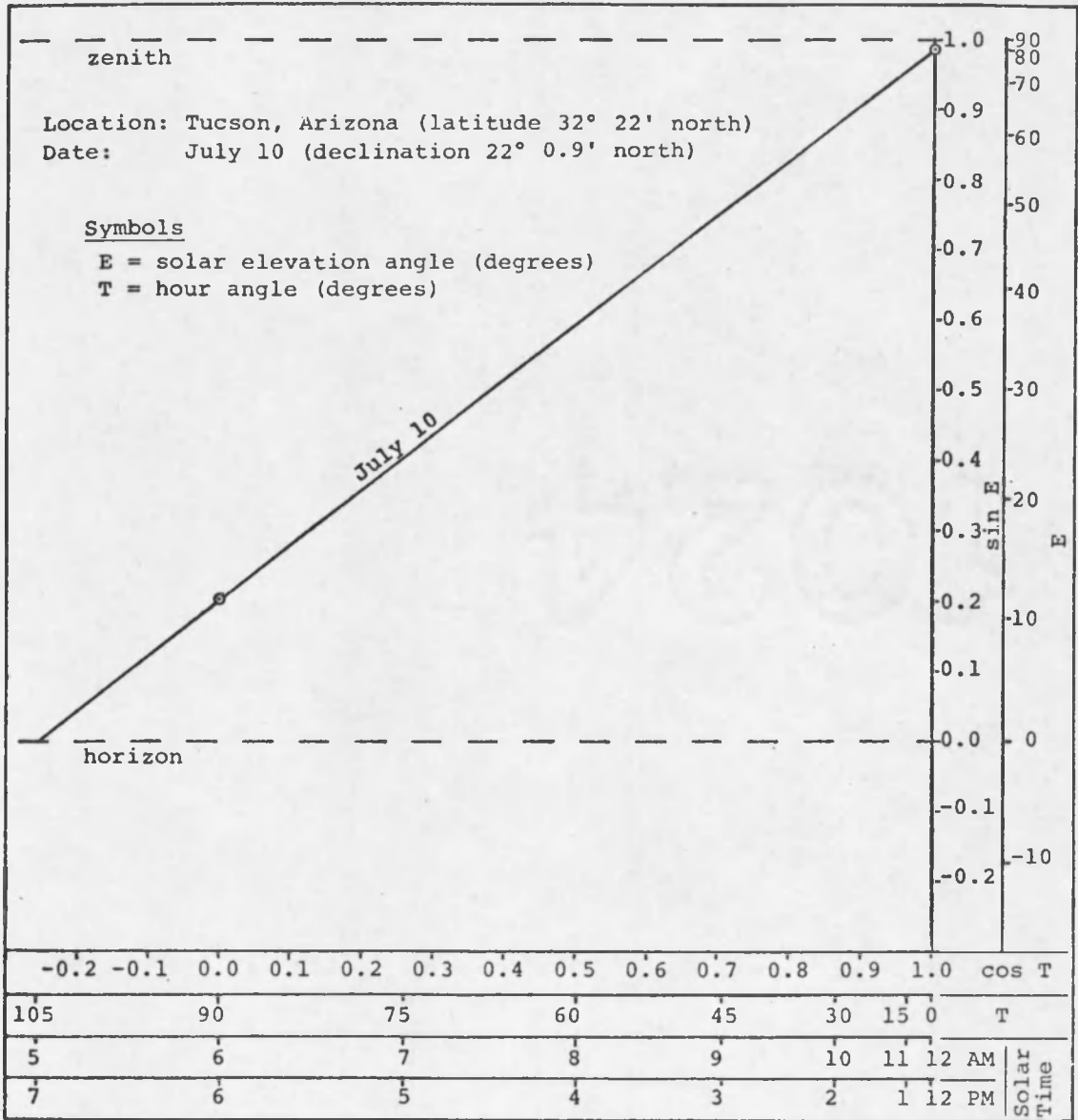


Figure 15. Solar elevation angle vs. time: Tucson, July 10

Table 1. Solar radiation data: Tucson, Ariz., July 10, 1974\*

(A) Apparent Solar Time		(B) E	(C) Raw Data (Qn)		(D) Qn	(E) Q	(F) Raw Data (Q+q)		(G) Q+q	(H) q
AM	PM		AM	PM			AM	PM		
5:02	6:58	0.0	0.00	0.00	0.00	0.00	0.00	0.01	0.00	0.00
05	55	0.7	0.00	0.00	0.12	0.00	0.00	0.02	0.01	0.01
10	50	1.7	0.05	0.35	0.26	0.01	0.01	0.04	0.02	0.01
20	40	3.3	0.40	0.48	0.45	0.03	0.04	0.06	0.05	0.02
30	30	5.3	0.56	0.60	0.58	0.06	0.07	0.09	0.09	0.03
40	20	7.3	0.69	0.72	0.69	0.09	0.11	0.12	0.13	0.04
50	10	9.4	0.80	0.81	0.78	0.13	0.15	0.16	0.18	0.05
6:00	6:00	11.4	0.87	0.88	0.85	0.17	0.19	0.20	0.22	0.05
10	50	13.4	0.93	0.94	0.91	0.21	0.23	0.24	0.27	0.06
20	40	15.3	1.00	1.00	0.97	0.26	0.28	0.28	0.32	0.06
30	30	17.4	1.06	1.04	1.02	0.30	0.33	0.33	0.37	0.07
40	20	19.4	1.11	1.08	1.07	0.36	0.37	0.37	0.43	0.07
50	10	21.5	1.15	1.12	1.11	0.41	0.42	0.42	0.48	0.07
7:00	5:00	23.5	1.18	1.17	1.14	0.45	0.46	0.48	0.53	0.08
10	50	25.5	1.21	1.18	1.17	0.50	0.51	0.53	0.58	0.08
20	40	27.7	1.24	XX	1.20	0.55	0.56	0.56	0.63	0.08
30	30	29.7	1.26	XX	1.22	0.60	0.60	0.63	0.69	0.09
40	20	31.7	1.28	XX	1.24	0.65	0.65	0.69	0.74	0.09
50	10	33.8	1.30	XX	1.26	0.70	0.68	0.73	0.79	0.09
8:00	4:00	35.9	1.31	1.27	1.28	0.75	0.73	0.78	0.84	0.09
10	50	38.0	1.33	1.29	1.29	0.80	0.78	0.80	0.89	0.09
20	40	40.1	1.35	1.33	1.31	0.84	0.82	0.85	0.94	0.10
30	30	42.2	1.36	1.34	1.32	0.89	0.86	0.88	0.99	0.10
40	20	44.4	1.37	1.35	1.33	0.93	0.90	0.89	1.03	0.10
50	10	46.5	1.38	1.37	1.34	0.97	0.94	0.93	1.07	0.10
9:00	3:00	48.6	1.39	1.39	1.35	1.01	0.97	0.96	1.11	0.10
10	50	50.8	1.40	1.40	1.36	1.05	1.02	0.99	1.15	0.10
20	40	53.0	1.41	1.41	1.37	1.09	ZZ	1.03	1.19	0.10
30	30	55.1	1.42	1.42	1.37	1.12	ZZ	1.06	1.22	0.10
40	20	57.1	1.43	1.43	1.38	1.16	ZZ	1.09	1.26	0.10
50	10	59.3	1.44	1.43	1.38	1.19	ZZ	1.12	1.29	0.10
10:00	2:00	61.5	1.44	1.44	1.39	1.22	ZZ	1.14	1.32	0.10
10	50	63.5	1.44	1.44	1.39	1.24	1.17	1.17	1.34	0.10
20	40	65.5	1.44	1.45	1.39	1.27	1.18	1.19	1.37	0.10
30	30	67.4	1.45	1.45	1.40	1.29	1.20	1.21	1.39	0.10
40	20	69.3	1.45	1.46	1.40	1.31	1.23	1.23	1.41	0.10
50	10	71.2	1.45	1.46	1.40	1.33	1.25	1.24	1.43	0.10
11:00	1:00	72.8	1.44	1.46	1.40	1.35	1.26	1.26	1.45	0.10
10	50	74.2	1.44	1.46	1.40	1.36	1.26	1.27	1.46	0.10
20	40	75.8	1.44	1.46	1.41	1.37	1.27	1.28	1.47	0.10
30	30	77.0	1.44	1.45	1.41	1.38	1.28	1.28	1.48	0.10
40	20	78.3	1.45	1.46	1.41	1.38	1.28	1.28	1.48	0.10
50	10	79.1	1.45	1.46	1.42	1.39	1.29	1.29	1.49	0.10
12:00	12:00	80.0	1.47	1.47	1.42	1.39	1.29	1.29	1.49	0.10

Table 1, continued

---

\*Explanation of column headings

- (B) E = solar elevation angle (degrees). Data from Figure 15.
- (C)  $Q_n$  = direct solar radiation rate on a normal plane (ly/min). Raw data from pyrliometer records, Institute of Atmospheric Physics, University of Arizona. In PM records, XX indicates sun obscured by clouds.
- (D)  $Q_n$  data after calibration correction and subsequent smoothing in Figure 16. Instrument calibration factor =  $0.968 \times (Q_n \text{ raw data})$ .
- (E) Q = (calculated) direct solar radiation rate on horizontal plane (ly/min).  $Q = Q_n \times \sin E$ .
- (F)  $Q+q$  = total (direct and diffuse) solar radiation rate on horizontal plane (ly/min). Raw data from pyranometer records, Institute of Atmospheric Physics, University of Arizona. In AM records, ZZ indicates a gap in the record.
- (G)  $Q+q$  data after calibration correction and subsequent smoothing in Figure 16. Instrument calibration factor =  $1.15 \times (Q+q \text{ raw data})$ .
- (H) q = (calculated) diffuse solar radiation rate on horizontal plane (ly/min).  $q = (Q+q) - Q$ .

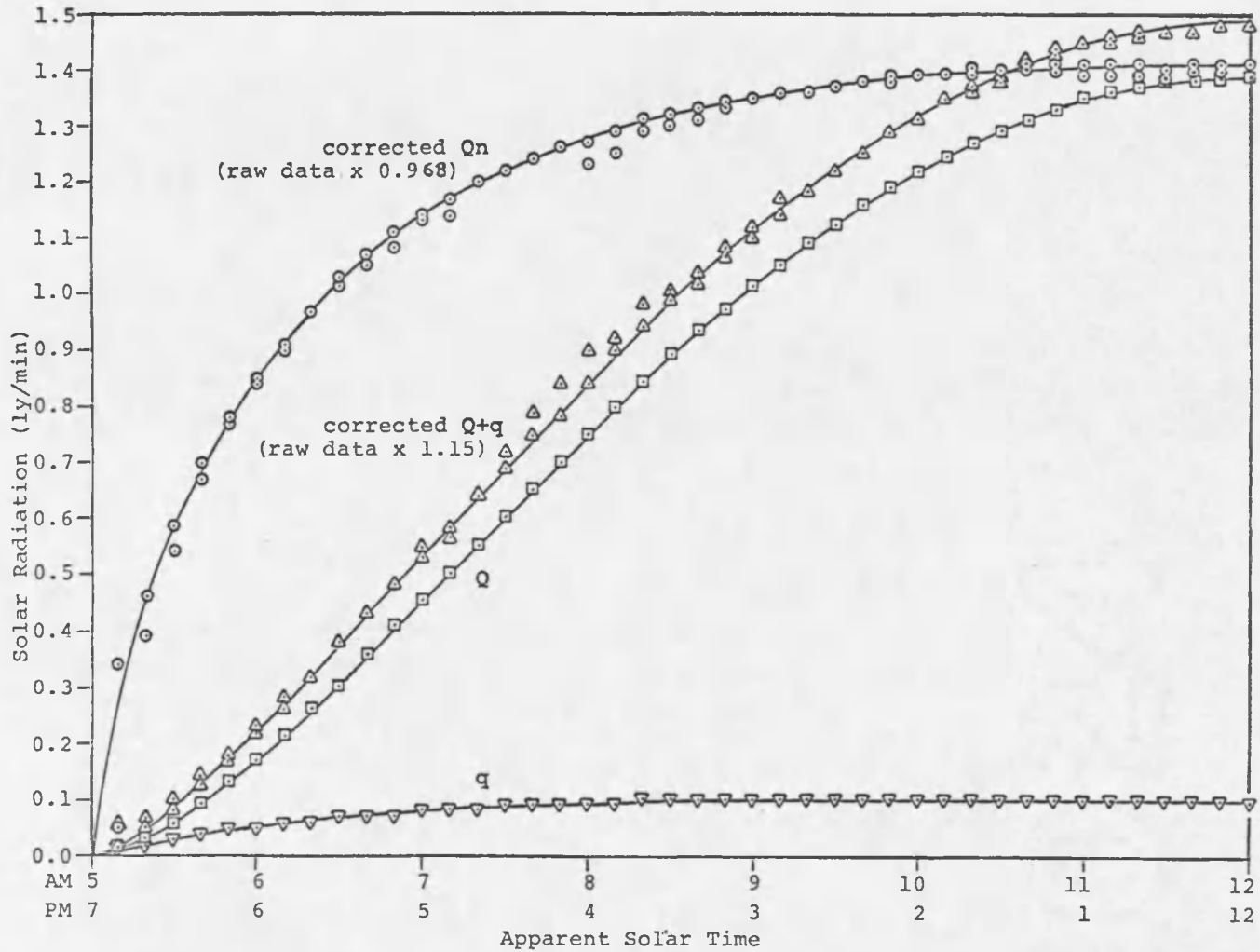


Figure 16. Solar radiation parameters vs. time: Tucson, Ariz., July 10, 1974

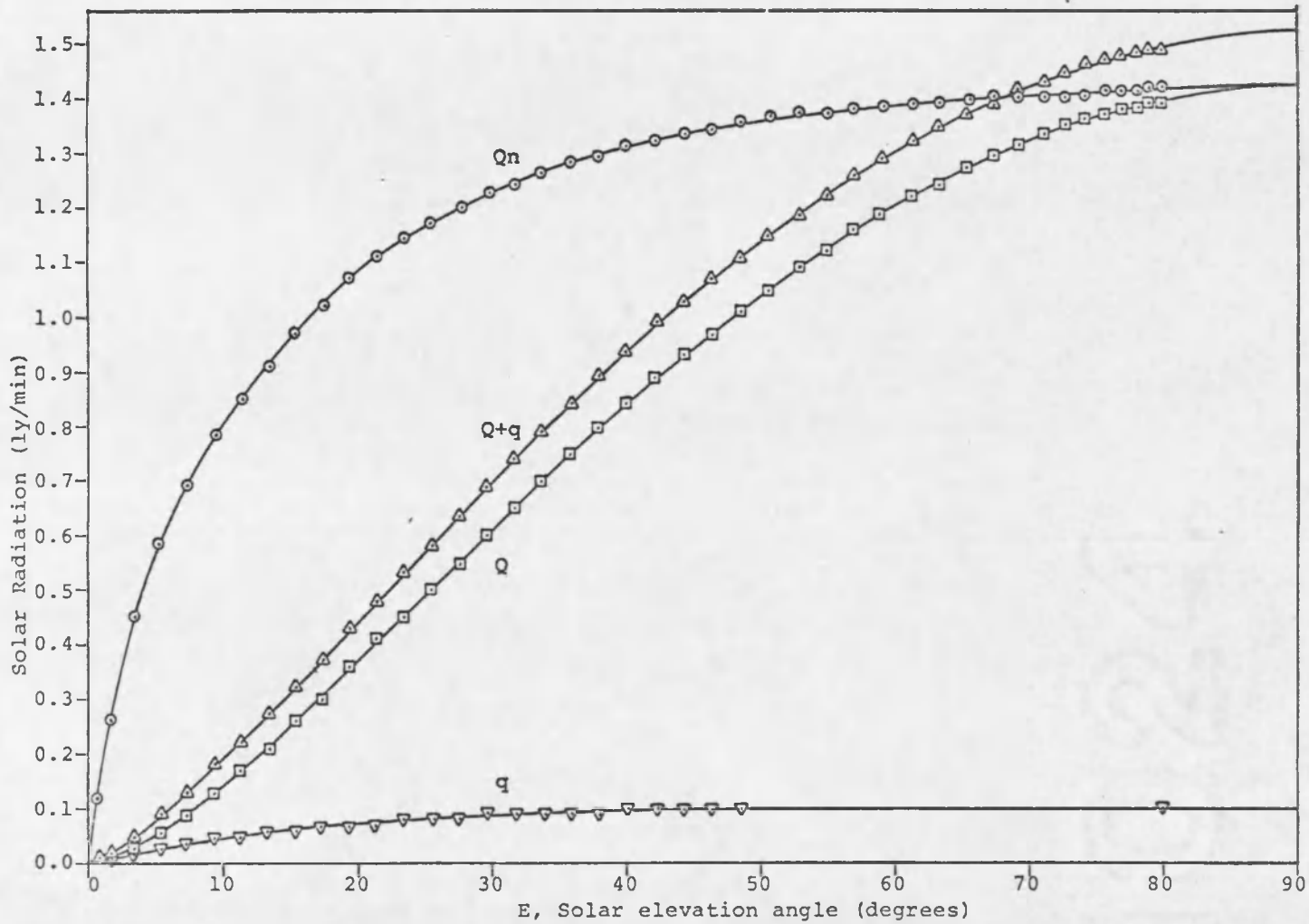


Figure 17. Solar radiation parameters vs. solar elevation angle: general model

Table 2. Solar radiation parameter values for selected solar elevation angles

E (°)	$Q_n$ $\frac{ly}{min}$	$Q$ $\frac{ly}{min}$	$Q+q$ $\frac{ly}{min}$	$q$ $\frac{ly}{min}$
0	0.00	0.00	0.00	0.00
5	0.57	0.05	0.07	0.02
10	0.80	0.14	0.19	0.05
15	0.96	0.25	0.31	0.06
20	1.08	0.37	0.44	0.07
25	1.16	0.49	0.57	0.08
30	1.23	0.62	0.71	0.09
35	1.28	0.73	0.82	0.09
40	1.31	0.84	0.94	0.10
45	1.34	0.95	1.05	0.10
50	1.36	1.04	1.14	0.10
55	1.37	1.12	1.22	0.10
60	1.38	1.20	1.30	0.10
65	1.39	1.26	1.36	0.10
70	1.40	1.32	1.42	0.10
75	1.41	1.36	1.46	0.10
80	1.42	1.40	1.50	0.10
85	1.42	1.41	1.51	0.10
90	1.42	1.42	1.52	0.10

## APPENDIX B

### SOLAR RADIATION MODEL FOR MOHAWK MOUNTAINS

Once a general clear-sky solar radiation model has been derived (Appendix A), only a few additional steps are needed to determine theoretical insolation curves for the Mohawk Mountains at monthly intervals.

Figure 18 was constructed to convert solar elevation angle data to specific time data for monthly sun paths at 32° north latitude. The same technique which produced Figure 15 was used. Latitude 32° north was chosen because a sun path diagram was available for it (Sellers 1965), although the Mohawk Mountains study area is actually closer to 33° north. For a pilot study the difference is negligible.

Values of  $Q$  (direct solar radiation on a horizontal surface) from Table 2 are plotted versus solar time (converted from solar elevation angle in Figure 18) to produce Figure 19.

For any time interval in Figure 19, the area under a curve (time integral) represents total direct solar radiation (energy) on a unit horizontal surface during that period. The units are langleys ( $1y = \text{cal}/\text{cm}^2$ ), energy per unit surface area.

Using a planimeter, cumulative areas under each curve were measured from time of sunrise/sunset (where  $Q = 0$ ) to points at half hour intervals. The data, when converted to ly units, represent values of  $Q_t$ , the cumulative direct solar radiation daily on a horizontal surface after sunrise or before sunset.  $Q_t$  is the parameter used to calibrate shadow dial and shadow maps in the Mohawk Mountains study (Chapter 4). These  $Q_t$  values are plotted against time in Figure 20.

Finally, for each  $Q_t$  value of the geometric series used in Chapter 4, apparent solar time and cumulative time after sunrise or before sunset (read from Figure 20) and solar elevation angle  $E$  (read from Figure 18) are listed in Table 3. This table can be used in interpreting Figures 6 through 13, the Mohawk Mountains solar shadow maps.

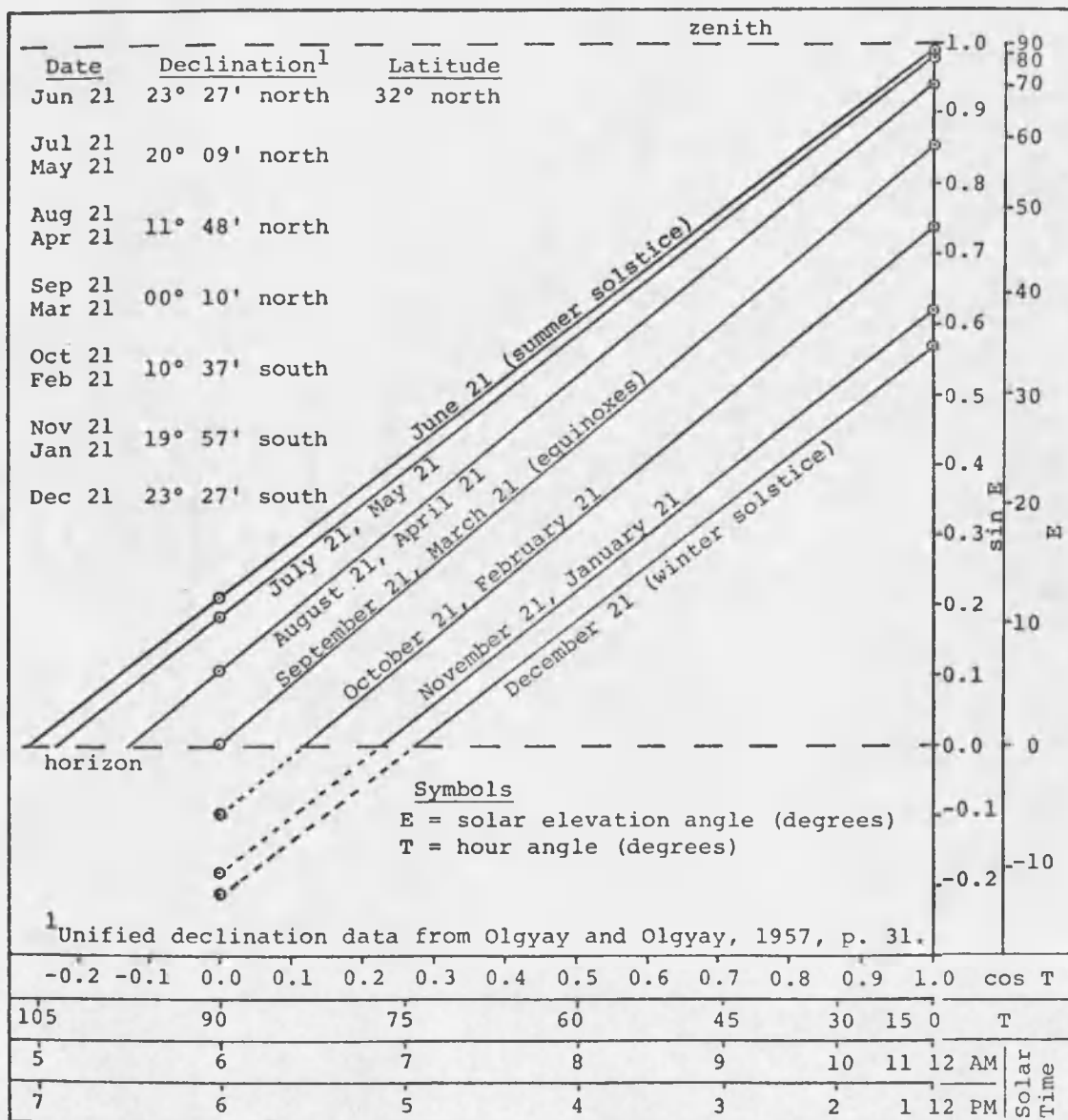


Figure 18. Solar elevation angle vs. time: monthly curves, 32° north

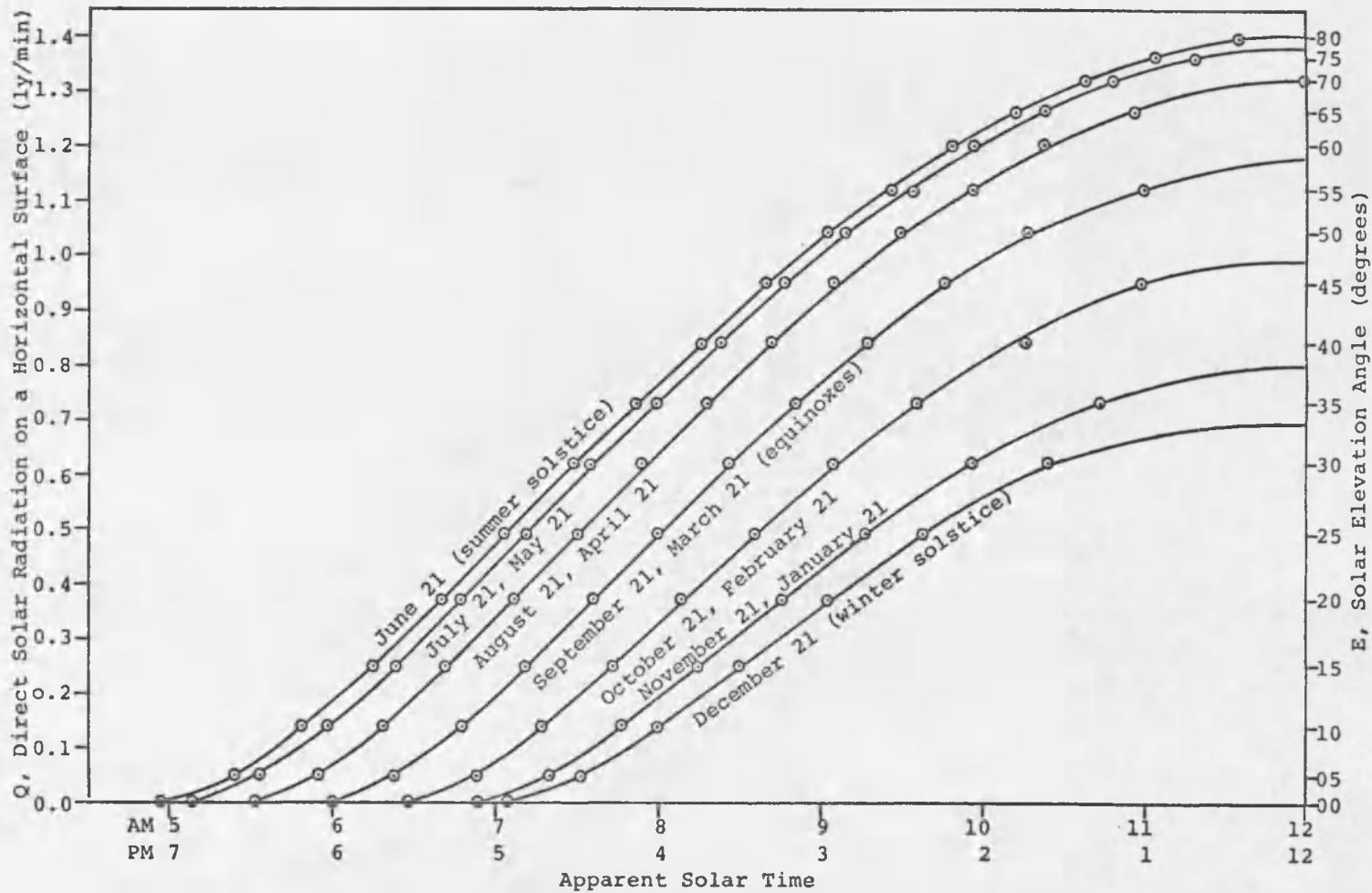


Figure 19. Direct solar radiation (Q) vs. time: monthly curves, 32° north

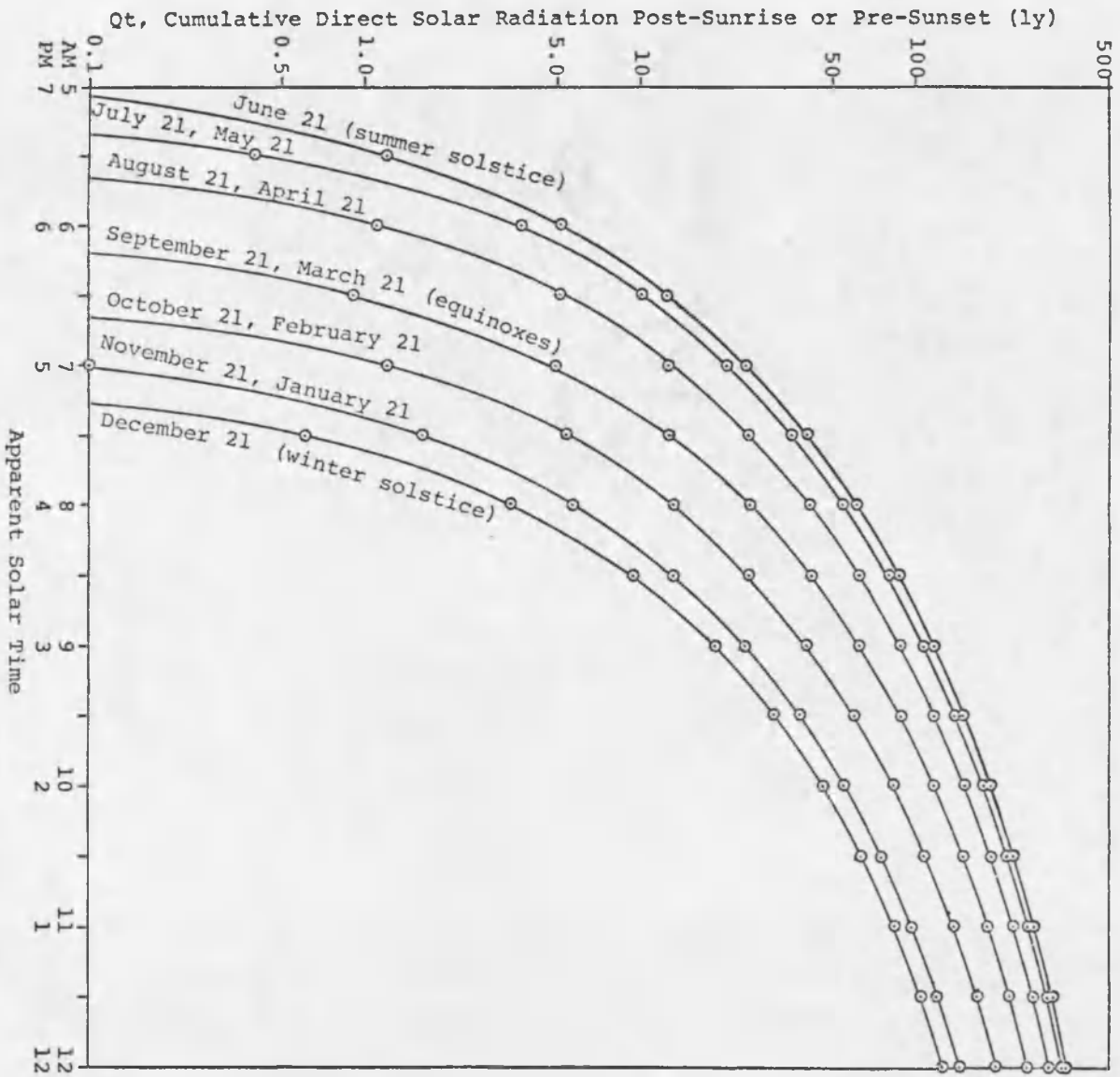


Figure 20. Cumulative direct solar radiation vs. time: monthly curves, 32° north

Table 3. Elevation angles and times for selected Qt values

Qt (ly)	E (°)	Apparent Solar Time		Cumulative Time Post- Sunrise or Pre-Sunset
		AM	PM	
JUNE 21 (summer solstice)				
64	38	8:06	3:54	3:09
32	28	7:18	4:42	2:21
16	21	6:45	5:15	1:48
8	15	6:15	5:45	1:18
4	11	5:54	6:06	0:57
2	8	5:39	6:21	0:42
1	6	5:29	6:31	0:32
1/2	4	5:19	6:41	0:22
1/4	3	5:13	6:47	0:16
0	0	4:57	7:03	0:00
JULY 21, MAY 21				
64	38	8:13	3:47	3:05
32	28	7:25	4:35	2:17
16	21	6:52	5:08	1:44
8	15	6:23	5:37	1:15
4	11	6:02	5:58	0:54
2	8	5:48	6:12	0:40
1	6	5:38	6:22	0:30
1/2	4	5:28	6:32	0:20
1/4	3	5:23	6:37	0:15
0	0	5:08	6:52	0:00
AUGUST 21, APRIL 21				
64	38	8:32	3:28	3:01
32	28	7:45	4:15	2:14
16	21	7:11	4:49	1:40
8	15	6:43	5:17	1:12
4	11	6:24	5:36	0:53
2	8	6:09	5:51	0:38
1	6	5:59	6:01	0:28
1/2	4	5:50	6:10	0:19
1/4	3	5:45	6:15	0:14
0	0	5:31	6:29	0:00
SEPTEMBER 21, MARCH 21 (equinoxes)				
64	37	9:02	2:58	3:02
32	28	8:15	3:45	2:15
16	21	7:41	4:19	1:41
8	15	7:12	4:48	1:12
4	11	6:53	5:07	0:53
2	8	6:38	5:22	0:38
1	6	6:29	5:31	0:29
1/2	4	6:19	5:41	0:19
1/4	3	6:14	5:46	0:14
0	0	6:00	6:00	0:00

Qt (ly)	E (°)	Apparent Solar Time		Cumulative Time Post- Sunrise or Pre-Sunset
		AM	PM	
OCTOBER 21, FEBRUARY 21				
64	35	9:35	2:25	3:07
32	27	8:46	3:14	2:18
16	20	8:09	3:51	1:41
8	15	7:43	4:17	1:15
4	11	7:22	4:38	0:54
2	8	7:07	4:53	0:39
1	6	6:57	5:03	0:29
1/2	4	6:47	5:13	0:19
1/4	3	6:42	5:18	0:14
0	0	6:28	5:32	0:00
NOVEMBER 21, JANUARY 21				
64	32	10:13	1:47	3:19
32	25	9:17	2:43	2:23
16	19	8:40	3:20	1:46
8	14	8:10	3:50	1:16
4	11	7:53	4:07	0:59
2	8	7:36	4:24	0:42
1	6	7:26	4:34	0:32
1/2	4	7:15	4:45	0:21
1/4	3	7:09	4:51	0:15
0	0	6:54	5:06	0:00
DECEMBER 21 (winter solstice)				
64	31	10:35	1:25	3:30
32	24	9:31	2:29	2:26
16	18	8:49	3:11	1:44
8	14	8:24	3:36	1:19
4	11	8:06	3:54	1:01
2	8	7:48	4:12	0:43
1	6	7:37	4:23	0:32
1/2	4	7:26	4:34	0:21
1/4	3	7:20	4:40	0:15
0	0	7:05	4:55	0:00

## APPENDIX C

### TOTAL ENERGY BLOCKED BY SHADOWS

What is the magnitude of total energy blocked daily by shadows in the Mohawk Mountains study area? Figure 7, the shadow map for June 21 (summer solstice), was chosen as an example to show how this question can be answered.

For each shadow boundary in Figure 7, the area between it and the mountain front was measured with a planimeter and converted to square kilometers ( $\text{km}^2$ ). This area value is plotted in Figure 21 above the appropriate value of  $Q_t$  [direct solar radiation on a horizontal surface cumulatively blocked daily either after sunrise (AM) or before sunset (PM)]. Values for AM and PM shadows are plotted separately. The difference between them, an artifact of oblique mountain range orientation, is quite apparent.

Area under each curve in Figure 21 represents the total solar energy blocked by shadows on the piedmont during that half of the day. When area is measured by planimeter and converted to energy units, the following values are obtained: for AM shadows  $65 \times 10^{10}$  calories (cal) or 760 megawatt-hours (Mwh), for PM shadows  $22 \times 10^{10}$  cal or 260 Mwh. Daily total is  $87 \times 10^{10}$  cal or 1020 Mwh, equivalent to 42.5 megawatts of continuous power.

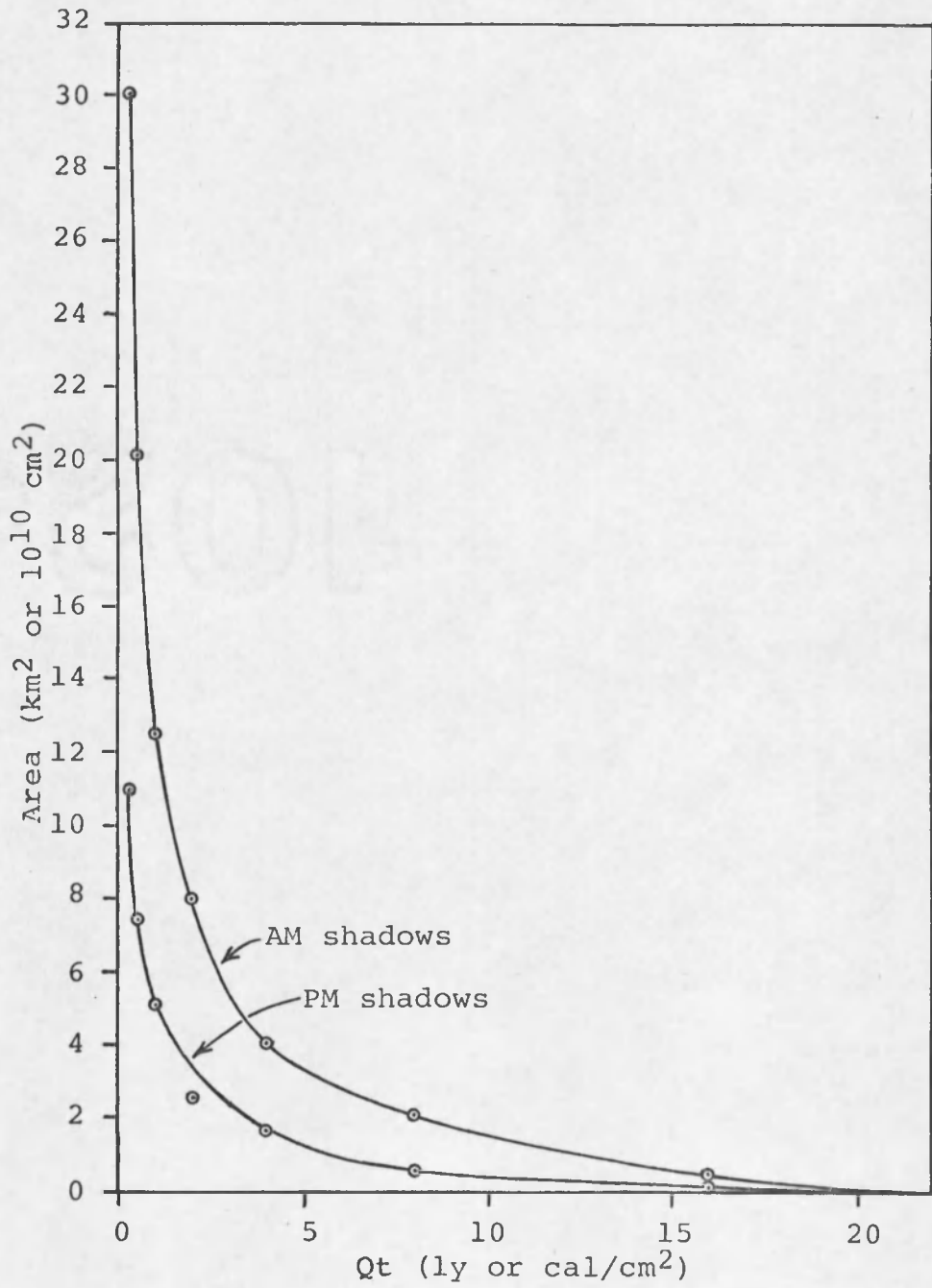


Figure 21. Area shaded vs. cumulative direct solar radiation blocked: June 21

## REFERENCES

- Abd el Rahman, A.A., and Batanouny, K.H., 1966, Micro-climatic conditions in Wadi Hoff: Société de Géographie d'Égypte, Bull., v. 39, p. 137-153.
- Anderson, H.W., and West, A.J., 1965, Snow accumulation and melt in relation to terrain in wet and dry years, in Washichek, J.N., ed., Proceedings, 33rd Annual Western Snow Conference: Colorado State Univ., Fort Collins, p. 73-82.
- Andrews, J.T., 1971, Quantitative analysis of the factors controlling the distribution of corrie glaciers in Okoa Bay, east Baffin Island, with particular reference to global radiation, in Morisawa, M., ed., Quantitative geomorphology: some aspects and applications: State Univ. of N.Y., Binghamton, Publications in Geomorph., p. 223-241.
- Aronin, J.E., 1953, Climate & architecture: New York, Reinhold Publ. Corp., 304 p.
- Babcock, H.M., Brown, S.C., and Hem, J.D., 1947, Geology and ground-water resources of the Wellton-Mohawk area, Yuma County, Arizona: U.S. Geol. Survey open file report, 22 p.
- Brown, G.W., 1970, Predicting the effect of clearcutting on stream temperature: Jour. Soil and Water Conservation, v. 25, no. 1, p. 11-13.
- Brum, G.D., 1973, Ecology of the saguaro (Carnegiea gigantea): phenology and establishment in marginal populations: Madrono, v. 22, no. 4, p. 195-204.
- Bryan, K., 1922, Routes to desert watering places in the Papago country, Arizona: U.S. Geol. Survey Water Supply Paper 490-D, p. 317-429.
- Bryan, K., 1925, The Papago country, Arizona, a geographic, geologic, and hydrologic reconnaissance, with a guide to desert watering places: U.S. Geol. Survey Water Supply Paper 499, 436 p.

- Buffo, J., Fritschen, L.J., and Murphy, J.L., 1972, Direct solar radiation on various slopes from 0 to 60 degrees north latitude: U.S. Forest Service, Pacific N.W. Forest and Range Expt. Sta., Portland, Oregon, Research Paper PNW-142, 74 p.
- Calandro, A.J., 1973, An analysis of stream temperatures in Louisiana: Louisiana Dept. of Public Works Technical Rept. 6, 16 p.
- Darton, N.H., 1933, Southern Pacific guidebook: U.S. Geol. Survey Bulletin 845, 304 p.
- Dean, J.S., 1969, Chronological analysis of Tsegi phase sites in northeastern Arizona: Univ. of Ariz. Press, Lab. of Tree-Ring Research Paper 3, 207 p.
- Despain, D.G., 1967, The survival of saguaro (Carnegiea gigantea) seedlings on soils of differing albedo, cover, and temperature [M.S. thesis]: Univ. of Ariz., 57 p.
- Dingman, S.L., and Koutz, F.R., 1974, Relations among vegetation, permafrost, and potential insolation in central Alaska: Arctic and Alpine Research, v. 6, no. 1, p. 37-42.
- Fons, W.L., Bruce, H.D., and McMasters, A., 1960, Tables for estimating direct beam solar irradiation on slopes at 30° to 46° latitude: U.S. Forest Service, Pacific S.W. Forest and Range Expt. Sta., Berkeley, Calif., 298 p.
- Fuggle, R.G., 1970, A computer programme for determining direct short-wave radiation income on slopes: McGill Univ., Climatological Bull., no. 7, p. 8-16.
- Fuggle, R.G., 1971, Relationships between micro-climatic parameters, and Basuto dwelling sites in the Marakabei Basin, Lesotho: So. African Jour. of Sci., v. 67, no. 9, p. 443-450.
- Garn, H.S., 1969, Factors affecting snow accumulation, melt, and runoff on an Arizona watershed [M.S. thesis]: Univ. of Ariz., 115 p.
- Garnett, A., 1935, Insolation, topography, and settlement in the Alps: Geographical Review, v. 25, no. 4, p. 601-617.
- Garnier, B.J., and Ohmura, A., 1968, A method of calculating direct shortwave radiation income of slopes: Jour. Applied Meteorol., v. 7, no. 5, p. 796-800.

- Garnier, B.J., and Ohmura, A., 1969, Estimating the topographic variations of short-wave radiation income: the example of Barbados: McGill Univ., Dept. of Geog., Climatological Research Series, no. 6, 66 p.
- Garnier, B.J., and Ohmura, A., 1970, The evaluation of surface variations in solar radiation income: Solar Energy, v. 13, no. 1, p. 21-34.
- Geiger, R., 1965, Climate near the ground: Harvard Univ. Press, 611 p.
- Geiger, R., 1969, Topoclimates, in Flohn, H., ed., General climatology: Amsterdam, Elsevier Publ. Co., v. 2, p. 105-117.
- Gibbs, J.G., and Patten, D.T., 1970, Plant temperatures and heat flux in a Sonoran Desert ecosystem: Oecologia, v. 5, no. 3, p. 165-184.
- Hamilton, W.J., III, 1971, Competition and thermoregulatory behavior of the Namib Desert tenebrionid beetle genus Cardiosis: Ecology, v. 52, no. 5, p. 810-822.
- Hellwig, D.H.R., 1973, Evaporation of water from sand, 1: experimental set-up and climatic influences: Jour. Hydrology, v. 18, no. 2, p. 93-108.
- Hendrick, R. L., Filgate, B.D., and Adams, W.M., 1971, Application of environmental analysis to snowmelt: Jour. of Applied Meteorology, v. 10, no. 3, p. 418-429.
- Hinds, W.T., and Richard, W.H., 1968, Soil temperatures near a desert steppe shrub: Northwest Sci., v. 42, no. 1, p. 5-13.
- Hogg, W., 1917, The book of old sundials & their mottoes: London, T.N. Foulis, 103 p.
- Hohauser, S., 1970, Architectural and interior models, design and construction: New York, Van Nostrand Reinhold Co., 211 p.
- Horton, J.S., 1966, Problems of land management in the various phreatophyte zones: Meeting of the Pacific Southwest Interagency Committee, Albuquerque, N.M., Aug. 30, 1966, 6 p.
- Hosni, S., 1971, SHADOW, a computer program for context response: Univ. of Oregon, Ctr. for Environmental Research, 37 p.

- Ives, R.L., 1962, Kiss tanks: *Weather*, v. 17, p. 194-196
- Knowles, R. L., 1969, Owens Valley study, a natural ecological framework for settlement: Univ. of S. Calif, Los Angeles, Dept. of Architecture, 85 p.
- Knowles, R.L., 1974, Energy and form, an ecological approach to urban growth: Cambridge, Mass., MIT Press, 198 p.
- Koutz, F.R., and Slaughter, C.W., 1973, Equivalent latitude (potential insolation) and a permafrost environment: Caribou-Poker Creeks research watershed, interior Alaska: Hanover, N.H., U.S. Army Corps of Engineers, Cold Regions Research and Engineering Lab Technical Note, 33 p.
- Lecarpentier, M., 1974, Développement d'un procédé numérique pour le calcul automatique des pentes et de leur insolation (Development of a numerical procedure for automatic calculation of slopes and their insolation): McGill Univ., Climatological Bull., no. 15, p. 1-10.
- Lee, R., 1963, Evaluation of solar beam irradiation as a climatic parameter of mountain watersheds: Colo. State Univ., Fort Collins, Hydrology Paper 2, 50 p.
- Lee, R., 1964, Potential insolation as a topoclimatic characteristic of drainage basins: *Internat. Assoc. of Scientific Hydrology Bull.*, v. 9, no. 1, p. 27-41.
- Lee, R., and Baumgartner, A., 1966, The topography and insolation climate of a mountainous forest area: *Forest Sci.*, v. 12, no. 3, p. 258-267.
- Lougeay, R., 1970, Microclimatological studies over the Seward Glacier snowpack, in Bushnell, V.C., and Rangle, R.H., eds., Icefield ranges research project scientific results: American Geographic Soc., New York, and Arctic Institute of North America, Montreal, v. 2, p. 17-26.
- Love, J., Jr., 1966, The development and evaluation of a shadow-photogrammetric method for determining the topography of an opaque surface [Ph.D. dissertation]: Okla. State Univ., 191 p.
- Lowe, C.H., and Hinds, D.S., 1971, Effect of paloverde (*Cercidium*) trees on the radiation flux at ground level in the Sonoran desert in winter: *Ecology*, v. 52, no. 5, p. 916-922.

- March, L., and Steadman, P., 1971, The geometry of environment: Cambridge, Mass., MIT Press, 360 p.
- Martsolf, J.D., Jr., 1966, Microclimatic modification through shade induced changes in net radiation [Ph.D. dissertation]: Univ. of Missouri, Columbia, 114 p.
- Matter, F.S., et al., 1974, A balanced approach to resource extraction and creative land development: Univ. of Ariz. College of Architecture and College of Mines, 85 p.
- Meehan, W.R., 1970, Some effects of shade cover on stream temperature in southeast Alaska: U.S. Forest Service, Pacific N.W. Forest and Range Expt. Sta., Research Note PNW-113, 9 p.
- Melton, M.A., 1960, Intravalley variation in slope angles related to microclimate and erosional environment: Geol. Soc. America Bull., v. 71, no. 2, p. 133-144.
- Nash, A.J., 1963, A method for evaluating the effects of topography on the soil water balance: Forest Science, v. 9, no. 4, p. 413-422.
- Ohmura, A., 1968, The computation of direct insolation on a slope: McGill Univ., Climatological Bull., no. 3, p. 42-53.
- Ohmura, A., 1970, The influence of the sky-line on the incidence of direct short-wave radiation: McGill Univ., Climatological Bull., no. 7, p. 17-24.
- Olgyay, A., and Olgyay, V., 1957, Solar control & shading devices: Princeton Univ. Press, 201 p.
- Ollier, C.D., 1969, Weathering: New York, American Elsevier Publ. Co., 304 p.
- Peel, R.F., 1960, Some aspects of desert geomorphology: Geography, v. 45, no. 4, p. 241-262.
- Pleijel, G., 1954, The computation of natural radiation in architecture and town planning [thesis]: Tekniska Hogskolan, Stockholm, 143 p.
- Pleijel, G., 1963, Swedish practices in window design, in Solar effects on building design: Washington, D.C., Building Research Institute, Publication 1007, p. 141-160.

- Puerto Rico Planning Board, 1969, The control of building shadow: same as author, 14 p.
- Randall, O.E., 1902, Shades and shadows and perspective: Boston, Ginn & Co., 64 p.
- Reid, I., 1973, The influence of slope orientation upon the soil moisture regime, and its hydrogeomorphological significance: Jour. Hydrology, v. 19, no. 4, p. 309-321.
- Reifsnyder, W.E., and Lull, H.W., 1965, Radiant energy in relation to forests: U.S. Forest Service, N.E. Forest Expt. Sta., Upper Darby, Pa., Technical Bull. 1344, 111 p.
- Reitan, C.H., and Green, C.R., 1968, Appraisal of research on weather and climate of desert environments, in McGinnies, W.G., Goldman, B.J., and Paylore, P., eds., Deserts of the world: Univ. of Ariz. Press, Office of Arid Lands Studies, p. 21-92.
- Robinson, N., 1966, Solar radiation: Amsterdam, Elsevier Publ. Co., 347 p.
- Rohr, R.R.J., 1965, Sundials--history, theory, and practice: Univ. of Toronto Press, 142 p.
- Ronco, F., 1970, Shading and other factors affect survival of planted Engelmann spruce seedlings in central Rocky Mountains: U.S. Forest Service, Rocky Mtn. Forest and Range Expt. Sta., Fort Collins, Colo., Research Note RM-163.
- Roth, E., 1965, Temperature and water content as factors in desert weathering: Jour. Geol., v. 73, no. 3, p. 454-468.
- Rouse, W.R., and Wilson, R.G., 1969, Time and space variations in the radiant energy fluxes over sloping forested terrain and their influences on seasonal heat and water balances at a middle latitude site: Geografiska Annaler, v. 51A, no. 3, p. 160-175.
- Sacamano, C.M., and Duffield, M.R., 1971, Arizona plant climate zones: Univ. of Ariz., Cooperative Extension Service, Q Series Arizona Garden Guides, 4 p.
- Sartz, R.S., 1972, Effect of topography on microclimate in southwestern Wisconsin: U.S. Forest Service, N.-Central Forest Expt. Sta., Research Paper RP-NC-74, 6 p.

- Seitz, W.C., 1960, Claude Monet, seasons and moments: New York, Museum of Modern Art, 64 p.
- Sellers, W.D., 1965, Physical climatology: Univ. of Chicago Press, 272 p.
- Shreve, F., 1931, Physical conditions in sun and shade: Ecology, v. 12, no. 1, p. 96-104.
- Snell, J.B., 1961, Method of predicting line-of-sight capabilities: preliminary investigations: Geol. Soc. America Bull., v. 72, no. 3, p. 479-484.
- Soons, J.M., and Rainer, J.N., 1968, Micro-climate and erosion processes in the southern Alps, New Zealand: Geografiska Annaler, v. 50A, no. 1, p. 1-15.
- Taylor, J.R., 1971, Model building for architects and engineers: New York, McGraw-Hill, 152 p.
- Thornthwaite, C.W., 1954, Topoclimatology, in Proceedings of Toronto meteorological conference, 1953: London, Royal Meteorological Society, p. 227-232.
- Tiedemann, A.R., Klemmedson, J.O., and Ogden, P.R., 1971, Response of four perennial southwestern grasses to shade: Jour. Range Management, v. 24, no. 6, p. 442-447.
- U.S. Army Map Service, 1960, Ajo, Arizona [plastic raised-relief topographic map, and regular topographic sheet]: U.S. Army Map Service, Map NI 12-10, horizontal scale 1:250,000, vertical scale 1:125,000, vertical exaggeration 2:1.
- Williams, L.D., Barry, R.G., and Andrews, J.T., 1972, Application of computed global radiation for areas of high relief: Jour. Appl. Meteorol., v. 11, no. 3, p. 526-533.
- Wilson, E.D., 1933, Geology and mineral deposits of southern Yuma County: Ariz. Bureau of Mines, Bull. 134, 236 p.
- Wilson, R.G., 1970, Topographic influences on a forest microclimate: McGill Univ. Climatological Research Series, no. 5, 109 p.

Wise, D.U., 1969a, Pseudo-radar topographic shadowing for detection of sub-continental sized fracture systems, in Proceedings, Sixth international symposium on remote sensing of environment: Univ. of Michigan, v. 1, p. 603-615.

Wise, D.U., 1969b, Regional and subcontinental sized fracture systems detectable by topographic shadowing techniques, in Baer, A., and Norris, D., eds., Proceedings, Conference on research in tectonics: Geol. Survey of Canada, paper 68-52, p. 175-199.

